Martin Brandauer
0530323

# Immobilization of cellobiose dehydrogenase on silicone catheters

MASTERARBEIT

zur Erlangung des akademischen Grades eines

Diplom-Ingenieurs

des Masterstudiums Biotechnologie

eingereicht an der

TECHNISCHEN UNIVERSITÄT GRAZ

Betreuer: Prof. Dr. Georg Gübitz

Institut für Umweltbiotechnologie

2013

# Abstract

This thesis was part of the NOVO project, which aimed at preventing microbial colonization and formation of biofilms on urinary silicone catheters. Microbial biofilms provide bacterial communities with protection from antibiotics and also cause approximately 40% of all infections in hospitals. This work therefore explores the possibility of creating catheters with cellobiose dehydrogenase (CDH) immobilized on the surface. The immobilized CDH will then use biofilm polysaccharides as its substrate to produce $H_2O_2$, which is lethal to bacteria. Several strategies were tested regarding the ability to immobilize CDH on silicone, including a layer by layer approach and an activation of the silicone surface followed by covalent attachment of CDH.

In the covalent immobilization approach, reactive hydroxyl groups were introduced onto the silicone surface. Two methods were used, one was the activation via the highly oxidative piranha solution and the other one was the activation via oxygen plasma gas. Following the activation of silicone a three-step process was performed. A silanization reaction with (3-aminopropyl)triethoxysilane (APTES) introduced amine groups onto the prior introduced hydroxyl groups. To finally bind CDH onto these amine groups glutaraldehyde was used as a crosslinker.

CDH was successfully immobilized with both methods. The layer by layer approach resulted in a $H_2O_2$ production of 14.4 µM after 3 hours of incubation. The covalently bound CDH produced 3.8 ± 0.3 µM $H_2O_2$ after 5 minutes of incubation.

The presented techniques offer the opportunity to produce antibacterial and antibiofilm catheters.

# Kurzfassung

Diese Arbeit war Teil des NOVO Projekts, welches versucht die mikrobielle Kolonisation und die Entstehung von Biofilmen auf Harnkathetern aus Silikon zu verhindern. Mikrobielle Biofilme schützen bakterielle Gemeinschaften gegen Antibiotika und sind verantwortlich für zirka 40% aller Infektionen in Krankenhäusern. Diese Masterarbeit sucht nach Möglichkeiten, Cellobiose Dehydrogenase (CDH) auf die Oberfläche von Silikonkathetern zu immobilisieren. CDH besitzt die Fähigkeit, Polysaccharide aus Biofilmen als Substrat zu verwenden und dadurch $H_2O_2$, welches tödlich für Bakterien ist, zu produzieren. Unterschiedliche Strategien für die Immobilisierung von CDH auf Silikon, wie die Layer-by-layer Technik und die Aktivierung von Silikon mit anschließender kovalenter Bindung von CDH, wurden getestet.

Für die Aktivierung und spätere Immobilisierung wurden reaktive Hydroxidgruppen in die Oberfläche von Silikon eingebracht. Zwei Methoden wurden dazu verwendet, eine Methode war die Aktivierung durch die stark oxidative Piranha Lösung, die zweite erfolgte durch Sauerstoffplasma Gas. Nach der Aktivierung wurde ein drei Schritt Prozess durchgeführt. Durch eine Silanisierungsreaktion mit (3-Aminopropyl)triethoxysilan (APTES) wurden Aminogruppen auf die vorher eingesetzten Hydroxidgruppen aufgebracht. CDH wurde dann mit Hilfe des Crosslinkers Glutaraldehyd auf diese Amingruppen gebunden.

Die CDH wurde mit beiden Methoden erfolgreich immobilisiert. Mittels der Layer-by-layer Technik produzierte die CDH 14,4 µM $H_2O_2$ nach 3 Stunden Inkubation. Die kovalent gebundene CDH produzierte 3,8 ± 0,3 µM $H_2O_2$ nach 5 Minuten Inkubation.

Diese Techniken bieten Möglichkeiten antibakterielle und Antibiofilm-Katheter zu produzieren.

*"Turn 180° and take a step forward"*

**(Yvon Chouinard)**

# Table of contents

# Table of Figures

# List of Tables

# 1 Introduction

## 1.1 Theoretical

### 1.1.1 The NOVO project

The NOVO project is funded by the European Union and has 11 beneficiaries. The main approach is the prevention and degradation of pathogenic bacteria biofilms formed on medical devices e.g catheters[1]. Biofilms are a hydrated polymeric matrix produced by bacterial communities. These self-encased bacteria have a strong resistance to the immune system and antibiotics, and makes it difficult-to-treat infections. Approximately 40% of all hospital infections are caused by biofilms which literally asks for a positive prevention of biofilm formation[2–6].

The NOVO project aims to develop a technical platform to prevent biofilm production on catheters via different approaches such as inorganic nanoparticles coating, enzymatically-generated antimicrobial phenolics and the immobilization of enzymes that use polysaccharides in biofilms as a substrate and produce $H_2O_2$ as an antibacterial agent[1]. To this end, our roll in the project is to develop enzyme based antimicrobial and antibiofilm systems. For this reason we investigated the possibility of using CDH immobilized on silicone catheter to act as an antimicrobial and antibiofilm agent.

### 1.1.2 Cellobiose dehydrogenase

Cellobiose Dehydrogenase (CDH) is an extracellular enzyme produced by wood degrading fungi. CDH belongs to the class of oxidoreductases. The enzyme consists of two domains, one bigger catalytically active domain that contains a flavin adenine dinucleotide (FAD) as a cofactor, and a smaller cytochrome b-type heme. They are connected via a protease sensitive linker region as shown in Figure 1[7,8].
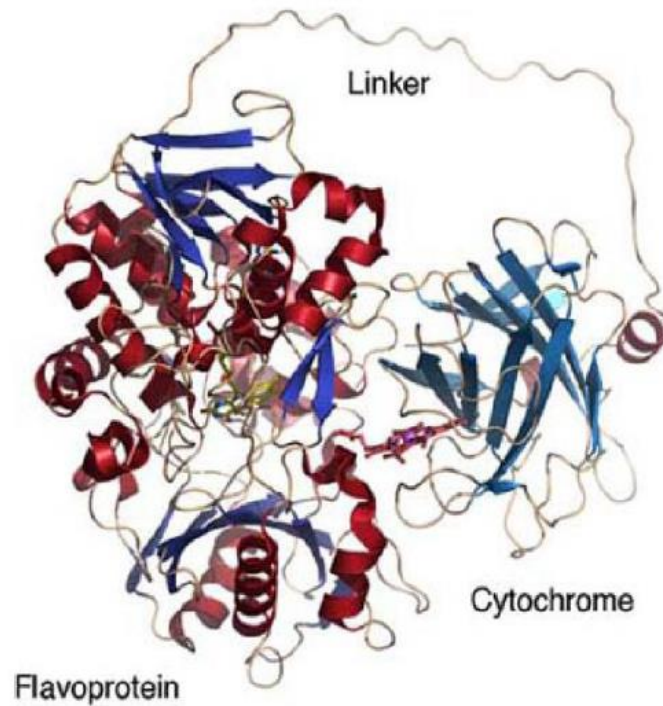


Figure 1: Structure of cellobiose dehydrogenase. The heme (cytochrome) domain and the FAD (flavoprotein domain are connected by a linker peptide[9]

CDH uses oligosaccharides like cellobiose, cellodextrines, mannodextrins, lactose and also cellulose as substrates (electron donors), and oxidizes them to their corresponding lactones by a ping-pong mechanism. The electrons can be transferred to a wide spectrum of electron acceptors including quinones, phenoxyradicals, $Fe^{3+}$, $Cu^{2+}$, triiodide ion and molecular oxygen. The reduction of oxygen results in the production of hydrogen peroxide[9] which is exploited in this study as an antimicrobial agent.

The catalytic mechanism can be divided in an oxidative and reductive half reaction. The oxidative reaction takes place at the C1 position of a saccharide. The hemiacetal at this position is converted to a lactone that converts spontaneously to a carboxylic acid under the presence of water. The mechanism of the first half reaction is shown in the Figure 2[9]:
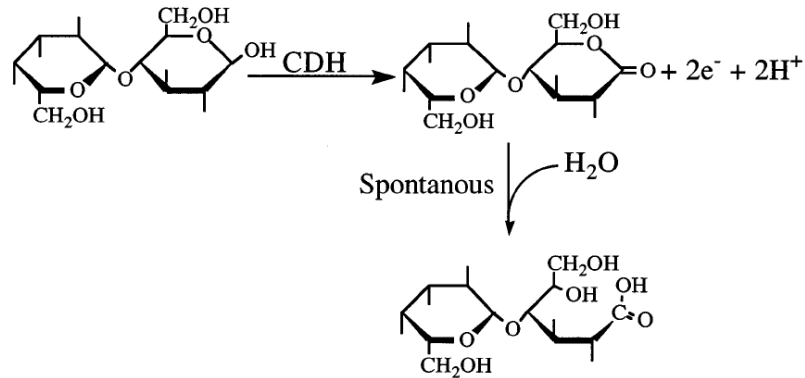
**Figure 2: Oxidative half reaction of cellobiose dehydrogenase**[9]

The two taken up electrons are then transferred to one two electron acceptor or two one electron acceptors as shown in Figure 3 and Figure 4[9].
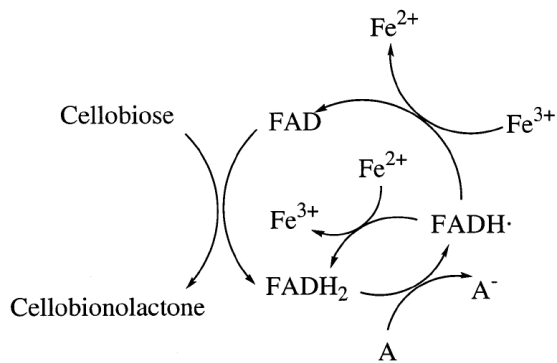


**Figure 3: Reductive half reaction of cellobiose dehydrogenase, electron transfer to one two electron acceptor**[9]
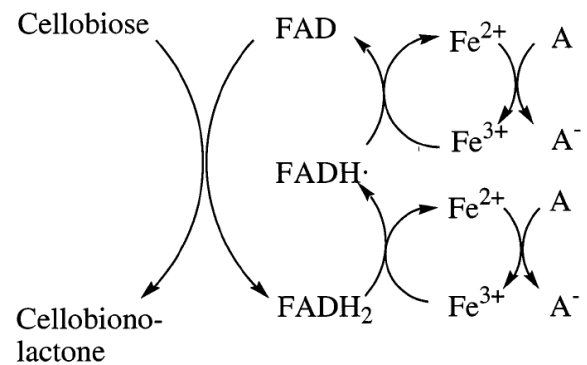


**Figure 4: Reductive half reaction of cellobiose dehydrogenase, electron transfer to two one electron acceptors**[9]

In nature CDH is part of a wood degrading process. The complex structure of higher plants makes them physically robust and chemically stable. Wood consists of cellulose microfibrils, which are embedded in a mixture of hemicellulose and lignin. This complex structure makes wood a difficult target for microbial degradation. CDH is able to bind to cellulose without loosing its catalytic ability. This concludes that the cellulose binding area is separated from the active site[10].

### 1.1.3  Biofilms

Biofilms result from an accumulation of microorganism on a surface. These microorganisms produce a polymeric matrix which mainly consists of extracellular polymeric substances (EPS) but also extracellular DNA, proteins and polysaccharides[11].

The formation of a biofilm can be divided into 5 stages as shown in Figure 5.
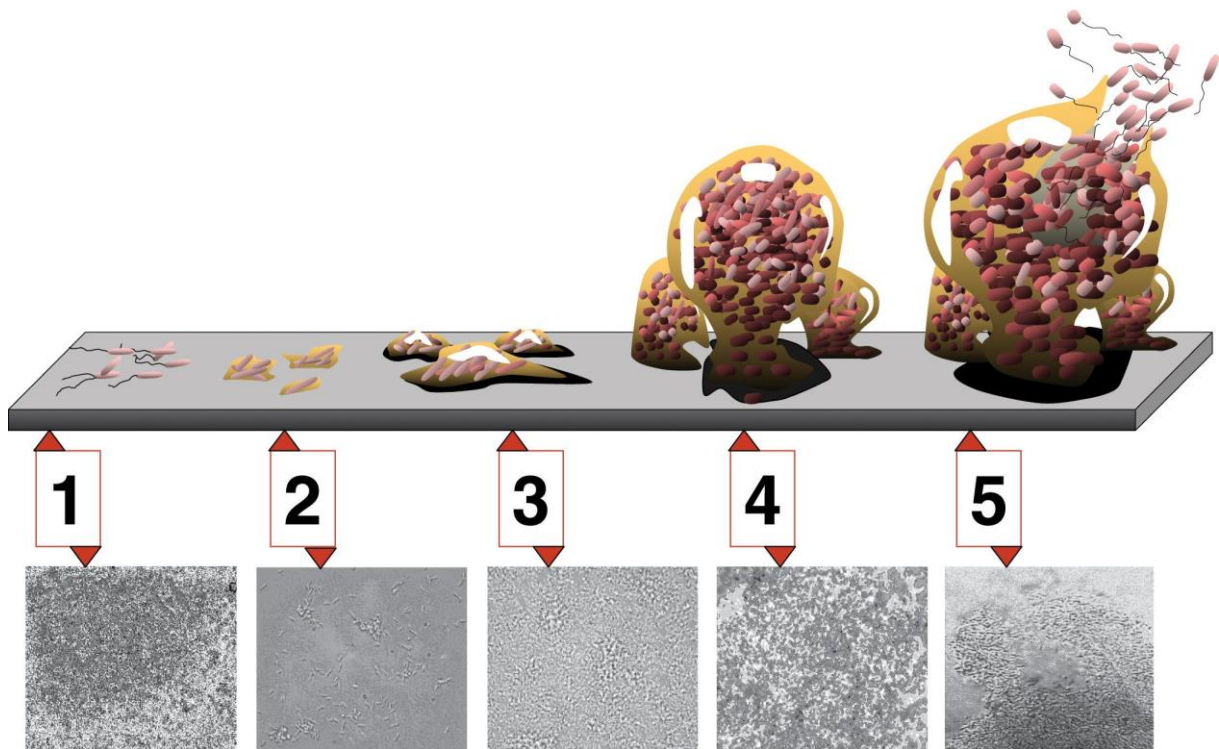


**Figure 5: Five stages of biofilm formation. (1) Initial attachment, (2) Irreversible attachment, (3) Maturation 1, (4) Maturation 2 and (5) Dispersion. Each stage of development in the diagram is paired with a photomicrograph of a developing P.aeruginosa biofilm. All photomicrographs are shown to same scale. Image credit: D.Davis [12]**

At first free-floating microorganisms attach to a surface and adhere via weak reversible van der Waals forces. If the cells have some time to linger on the surface and aren't separated instantly, they are able to form a more stable anchor via cell adhesion. Some species are not able to attach to the surface on their own but are able to bind to the polymer matrix or other already bound colonists. Colonization leads to biofilm growth through cell division or recruitment. The last stage is the dispersion in which the biofilm is fixed and only changes in shape and size[13].

Biofilms are responsible for a significant amount of human microbial infections. Biofilms are mainly formed on implanted/indwelling medical devices which remain in a human body for a period of time. Microorganisms living in a biofilm community are very resistant to antibiotics because of the EPS matrix which acts like a protective covering. At the moment the only defense against these biofilms is to remove the medical device out of the body, which leads to higher costs. New approaches for detecting and controlling biofilms are needed[14].

### 1.1.4 Surface - immobilized enzymes

The immobilization of biomolecules such as enzymes, antibodies, cells and drugs is the directed manipulation of their mobility while maintaining their activity. This can be achieved via chemical and physical methods like adsorption, entrapment or covalent binding of the biomolecule on the desired material. Among the different materials, synthetic polymers are especially interesting because their surfaces contain reactive groups like –OH, -COOH or –$NH_2$ to covalently bind the molecule.

The main reasons for enzyme immobilization are easy separation of the enzyme from the product and the reuse of the enzyme after the process. The reuse of the enzyme also reduces the costs of the process. Other advantages and disadvantages of immobilized enzymes are combined in Table 1[15].

Table 1: Advantages and disadvantages of immobilized enzymes[15]

| Advantages | Disadvantages |
|---|---|
| Enhance stability | Difficult to sterilize |
| Can modify enzyme microenvironment | Fouling by other biomolecules |
| Can separate and reuse enzyme | Mass transfer resistance (substrate in product out) |
| Enzyme free product | Adverse biological response of enzyme surfaces |
| Lower cost, higher purity product | Greater potential for product inhibition |
| No immunogenic response (therapeutics) | |

As mentioned above the most important parameter throughout enzyme immobilization is that the enzyme remains its activity. Proteins are dynamic flexible molecules and often need to move in their natural environment to perform their reaction. To maintain this function throughout the immobilization process empirical guidelines and exact knowledge of the structural characteristics are essential. Regions that are essential for the catalytic mechanism should be conserved[16].

The binding methods differ between physical interactions and covalent binding. The purpose of the binding determines the method that is used. If the molecule needs to be attached permanently, covalent binding is the method of choice. On the other hand, in a drug delivery system, where the molecule has to be released after a certain amount of time, the physical method is more appropriate. Costs are an other determining factor for choosing a method, adsorption techniques are most of the times cheaper than covalent binding techniques[15]

There are three main techniques for immobilization[15]:

1. *Physical adsorption*: van der Waals forces, electrostatic interactions and affinity recognition. Through these interactions enzymes are able to adsorb to surfaces.

2. *Entrapment*: microcapsules, hydrogels and physical mixtures such as matrix drug delivery systems

3. *Covalent attachment*: soluble polymer conjugates on solid surfaces or conjugates within hydrogels

In Figure 6 immobilization methods are shown in more detail:
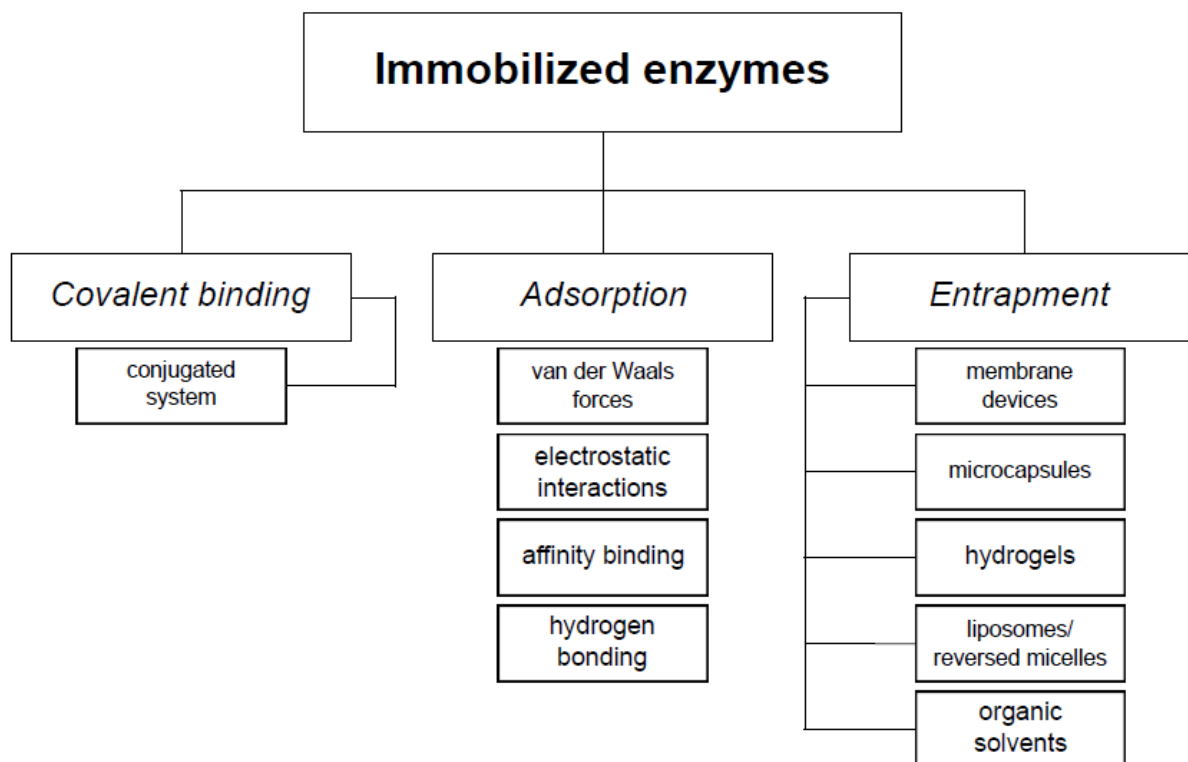


Figure 6: Different immobilization methods subdivided by their interactions

Adsorption is a reversible immobilization method and technically easy to perform. The interactions between the surface of the material and the enzyme are based on weak forces, but still enabling an efficient binding process. Van der Waals forces, ionic and hydrophobic interactions and hydrogen bonds belong to these interactions. They are very dependable on the conditions of the immobilization process. The pH value, the temperature and the ionic strength are very important and have to be controlled exactly - small changes can affect the binding process radically[17].

Entrapment is an irreversible immobilization technique, which traps the enzyme inside a matrix. A major drawback are the costs [17].

Another irreversible process is the covalent binding. To bind the enzyme covalently to a surface, the surface needs reactive groups which can interact with the molecule. If these groups are not available, the surface must be modified. There are a lot of modification techniques including chemical modification, plasma gas discharge, photochemical crafting and chemical derivatization. There is also the possibility to attach an enzyme to the surface with a spacer group or a linker. The linker connects the material with the enzyme [18–20].

Immobilizing enzymes increase the functional benefit of surfaces. New properties can be added which broadens the materials spectrum of use. For example urinary catheters are a common source for infections, and immobilizing enzymes is one approach for preventing these.

### 1.1.5 Urinary catheters

The word catheter comes from the Greek word for "send down"(αποβάλλω) translated in French "une catheter"[21]. A catheter is used in the treatment of urinary incontinence, a condition that affects the function of the bladder. A flexible hollow tube is inserted into the bladder via the urethra and stabilized via an inflatable balloon just under the drainage eye of the catheter. In Figure 7 a catheter with description is shown.
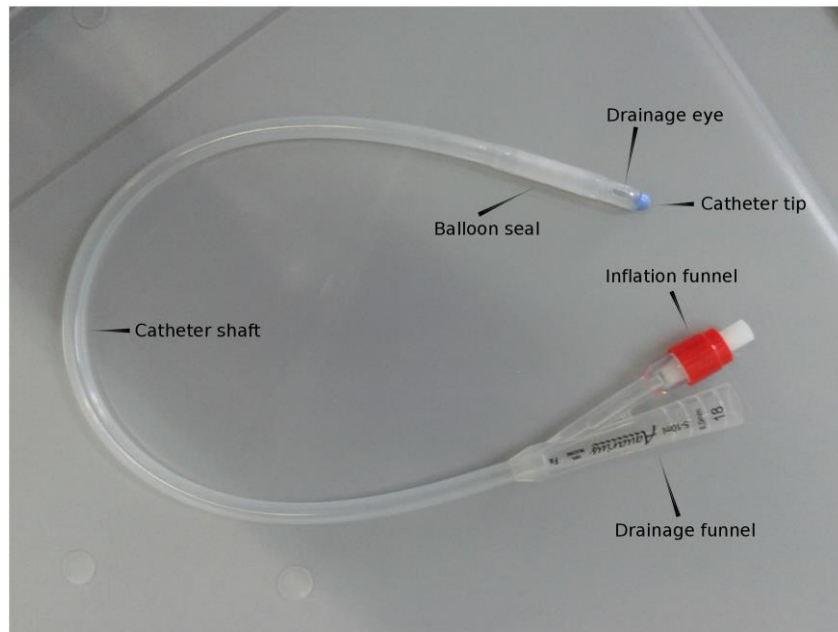


Figure 7: A Silicone catheter. Image credit: Barbara Thallinger

The material used for a catheter has to be biocompatible and convenient for its purpose. The physical and mechanical properties are essential[22]. Throughout the evolution of catheters a lot of materials came to use. From metals (silver-bronze) to animal skin to rubber and finally to latex and silicone[21].

As latex had to contend with allergies, some also life threatening such as anaphylaxis, silicone was getting more attention in the 20th century.

### 1.1.6    Polydimethylsiloxane (PDMS)

Polydimethylsiloxane is a polymeric organosilicon also known as silicone[23]. The chemical formula for PDMS is $[Si(CH_3)_2O]_n$ where n is the number of monomer units. Its structure is shown in Figure 8.
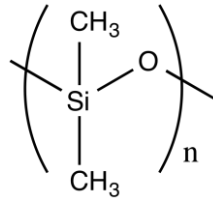


**Figure 8: Structure of polydimethylsiloxane**

PDMS is produced from silica ($SiO_2$) in a 4 step synthesis where the last steps are polymerization and polycondensation.  Silicone elastomers can easily create a three dimensional network through crosslinking between the polymer chains. The crosslinking has the purpose of decreasing flexibility, increasing the hardness and also increasing the melting point of the polymer[24].

The high stability of silicone is due to the highly ionic Si-O bond, which has a high bond energy. The methyl groups (-$CH_3$) are not interacting with each other and shield the main chain which leads to a low surface tension. The siloxane chain is configured in a way that the maximum number of methylgroups are exposed at the surface which results in very hydrdophobic surfaces[25]. PDMS is very permeable to oxygen, nitrogen or water vapor caused by the low intermolecular interactions that lead to a high free volume[26].

Silicone is very biocompatible, chemical inherent, very thermo stable (up to 230°Celsius, makes it easy to sterilize), has a low surface tension and a high hydrophobicity. Because of these properties silicone is the material of choice for a lot of medical products and catheters[27]. Though there is always room for improvement. The high rate of medical infections caused by silicone catheters, which remain in the body for a longer period of time, need to be addressed. There are many techniques investigated for developing antimicrobial and antibiofilm properties for catheters such as the layer by layer technique and also the covalent binding of proteins. Often the inert surface of PDMS has to be activated.

## 1.2 Strategies for the immobilization of bioactive molecules on biomaterials

### 1.2.1 Layer by Layer technique

The layer-by-layer technique is an easy adsorption technique to form multilayers on surfaces. The creation of multilayers is achieved through the alternating deposition of polyanions (negatively charged particles) and polycations (positive charges particles) on the support. Electrostatic interactions and/or hydrophobic interactions between them are responsible for the attachment. The deposition procedure is shown in Figure 9[28,29].
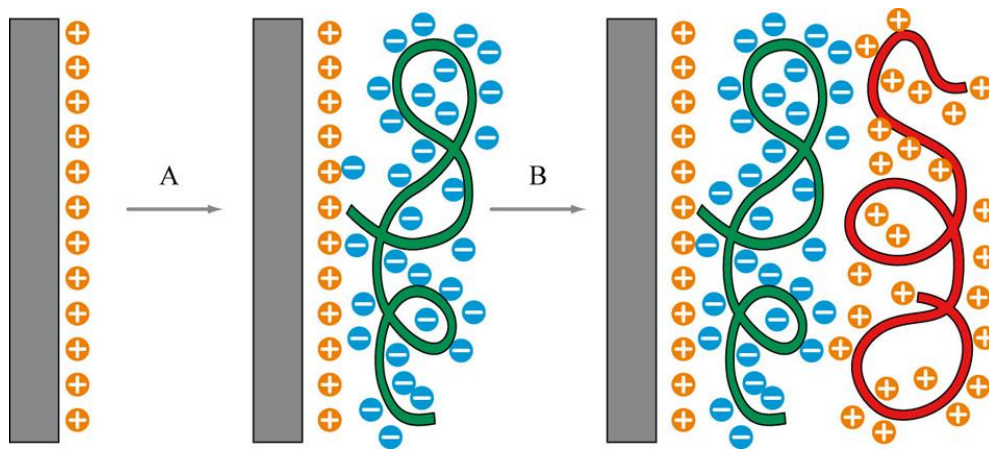


Figure 9: Layer by layer assembly[30]

The samples are dipped into the different solutions with washing steps in-between. For example +-+- are two bilayers with the polycation as the first layer and the polyanion as the top layer. With this procedure it is possibly to build up multilayer films.

Examples for positively charged polyelectrolytes are poly(diallyldimethylammonium chloride) (PDDA), poly(allylaminehydrochloride) (PAH), or polyethyleneimine (PEI) and Chitosan. Polyanions are poly(styrenesulfonate) (PSS), poly(vinyl sulfate), or poly(acrylic acid)[28].

### 1.2.2 Surface activation of PDMS

Due to the lack of reactive groups on the silicone surface, activation prior to the immobilization process is necessary. There are a lot of ways of introducing active groups to the surface, such as UV radiation, Plasma gas or chemical ways. Depending on the purpose and given requirements the right method must be selected. In this project reactive groups on the surface of PDMS are needed to immobilize CDH, to achieve this, radical methods like plasma gas or the highly oxidative piranha solution will be executed.

**Plasma Treatment**

Radio frequency glow discharge (RFGD) also called plasma is a treatment classified as a nonspecific chemical reaction, meaning that a variety of functional groups can be introduced on/into a surface[31]. Plasmas are atomically and molecularly dissociated gaseous environments. It contains ions, electrons, atoms, photons and molecules. A lot of reactions can take place on the substrates surface that lead to a modification, most frequently a deposition or an ablation happens. Those two compete, if the ablation is more rapid than the deposition, no deposition will be observed. The energetic nature of ablation can result in a chemical or morphological modification of the substrate. Either free radicals or reactive species in the gas environment can react with the surface, or molecules combine in the gas phase to particles of higher molecular weight settle to the surface[31].

In Figure 10 an apparatus to generate plasma is shown. The major components are a gas introduction system, a vacuum system, an energizing system and a reactor zone.
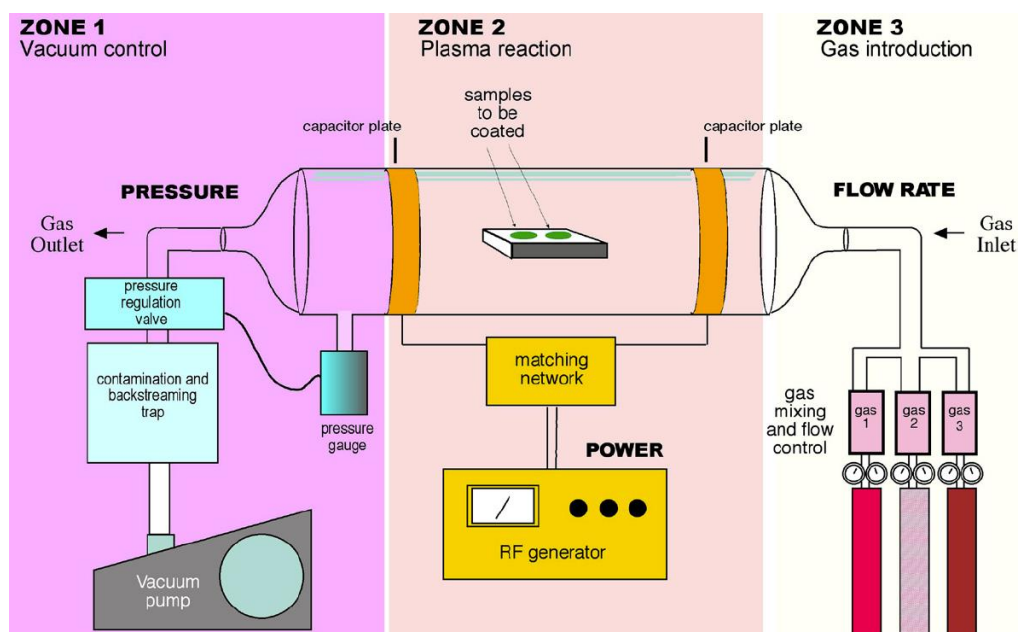


Figure 10: A Plasma apparatus. Zone 1 is the vacuum control system, Zone 2 the energizing system where the plasma reaction takes place and where the samples are placed, Zone 3 is gas introduction and control system[31]

In Table 2 different gases, depending on the wanted reactive group are shown.

Table 2: Different plasma gases with their corresponding reactive group[32]

| Gas | Reactive group |
| --- | --- |
| $N_2$, $NH_3$, $N_2/H_2$ | Amine groups $-NH_2$ |
| $CO_2$, $CO$ | Carboxy groups - COOH |
| $O_2$ | Hydroxy groups -OH |

### *1.1.8.2 Piranha solution*

Piranha solution is strong oxidizing agent composed of sulfuric acid ($H_2SO_4$) and hydrogen peroxide ($H_2O_2$) in different mixtures (3:1, 4:1, 7:1…). It is used to clean organic residues off substrates and it is a wet chemical way to add −OH groups to most surfaces and so activate them for further reactions like an enzyme immobilization.

The reaction mechanism of the piranha solution is divided in two coexistent processes. In the first reaction the sulfuric acid removes water and creates the so-called "Caros's Acid" ($H_2SO_5$) that is one of the strongest oxidants known and highly explosive, as shown in Equation 1.

Equation 1:

$$H_2SO_4 + H_2O_2 \rightarrow H_2SO_5 + H_2O$$
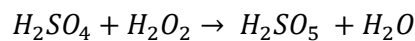
The second reaction is the transformation of the mild oxidizing agent hydrogen peroxide into a highly aggressive one, which is able to dissolve a very resistant elemental carbon. The dehydration of $H_2O_2$ forms hydronium ions, bisulfate ions and atomic oxygen as shown in Equation 2.

Equation 2:

$$H_2SO_4 + H_2O_2 \rightarrow H_3O^+ + HSO_4^- + O$$
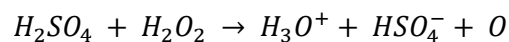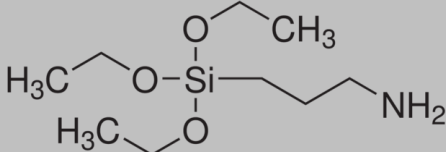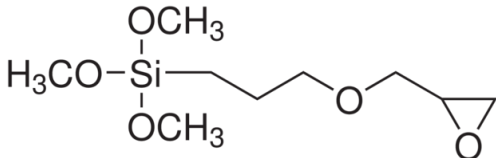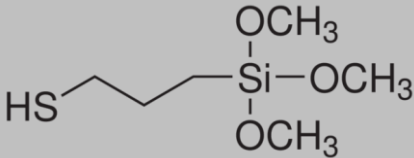
The extremely reactive oxygen is responsible that the piranha solution is able to attack highly stable carbon bonds on a surface.
The piranha solution is able to oxidize the methyl groups of PDMS, and introduce −OH groups to the surface.

### 1.2.3 Silanization

A silanization reaction is the covering of a hydroxylated surface with organofunctional alkoxysilanes. These reactions are easy to perform and of low cost. Organofunctional alkoxysilanes have a common atomic backbone with methoxy or ethoxy groups, but have different functional groups depending on the purpose[31]. Different alkoxysilanes with their functional group are shown in Table 3.

Table 3: Different alkoxysilanes. Structures from Sigma Aldrich

| Name | Structure |
|---|---|
| (3-Aminopropyl)triethoxysilane (APTES) |  |
| (3-Glycidyloxypropyl)trimethoxysilane) (GOPTMS) |  |
| (3-Mercaptopropyl)trimethoxysilane (MPTMS) |  |

The reaction mechanism for a silane surface modification consists of 4 reactions. The first step is the hydroxylation of the silane agent prior to the surface treatment. The hydroxylation creates a silanol group which can condense with other silanol groups from other organosilane molecules, to form siloxane linkages. The resulting oligomers are able to build up a hydrogen bond to the hydroxyl groups of the supports surface. The last step is the forming of a covalent bond between the surface and the organosilane, which happens due to temperature increase and the resulting loss of water[33]. The reaction mechanism for a silane surface modification with APTES is shown in Figure 11: APTES reaction mechanism. 1) Hydrolysis 2) Condensation 3) Hydrogen bonding with surface 4) covalent binding with surface. Mechanism according to [33].
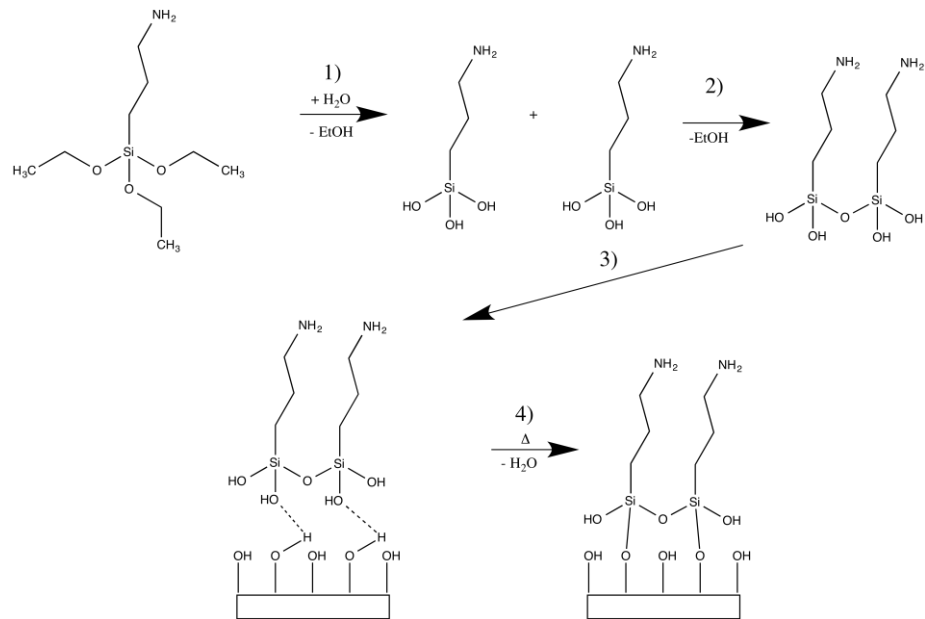
**Figure 11: APTES reaction mechanism. 1) Hydrolysis 2) Condensation 3) Hydrogen bonding with surface 4) covalent binding with surface. Mechanism according to [33].**

Silane reactions are very simple to perform but they are building a very stable crosslinked network on a surface. It helps adding different functional groups to a hydroxylated surface.

### 1.2.4    Glutaraldehyde

Glutaraldehyde is a protein crosslinking agent. It is a linear 5-carbon dialdehyde that is soluble in water alcohol and organic solvents. It reacts very fast with amine groups at a neutral pH value, and builds stable crosslinks. This fact makes it very useful for enzyme immobilizations[34]. In Figure 12 the structure of glutaraldehyde is shown.
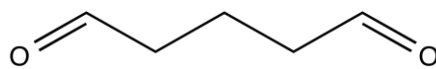


**Figure 12: Structure of glutaraldehyde**

### 1.2.5 Aim of work

The main goal of this work is the immobilization of cellobiose dehydrogenase (CDH) on silicone (polydimethylsiloxane). Two approaches, namely Layer by Layer and covalent binding, will be used to attach the enzyme to the surface. Applying the layer-by-layer technique with chitosan as a polycation and CDH as polyanion will be one approach and the other one will be, after activating PDMS surface via the piranha solution or plasma treatment, to covalently bind CDH. The reaction will be set up as a 4-step process. First the PDMS surface will be activated through hydroxyl group introduction. The next step will be a silanization reaction with APTES. Glutaraldehyde will be used as a crosslinker between the enzyme and the introduced amine groups, which will be the third step. The fourth step and last step will be the actual immobilization of CDH on the aldehyde groups of glutaraldehyde. These steps are simplified shown in Figure 13.
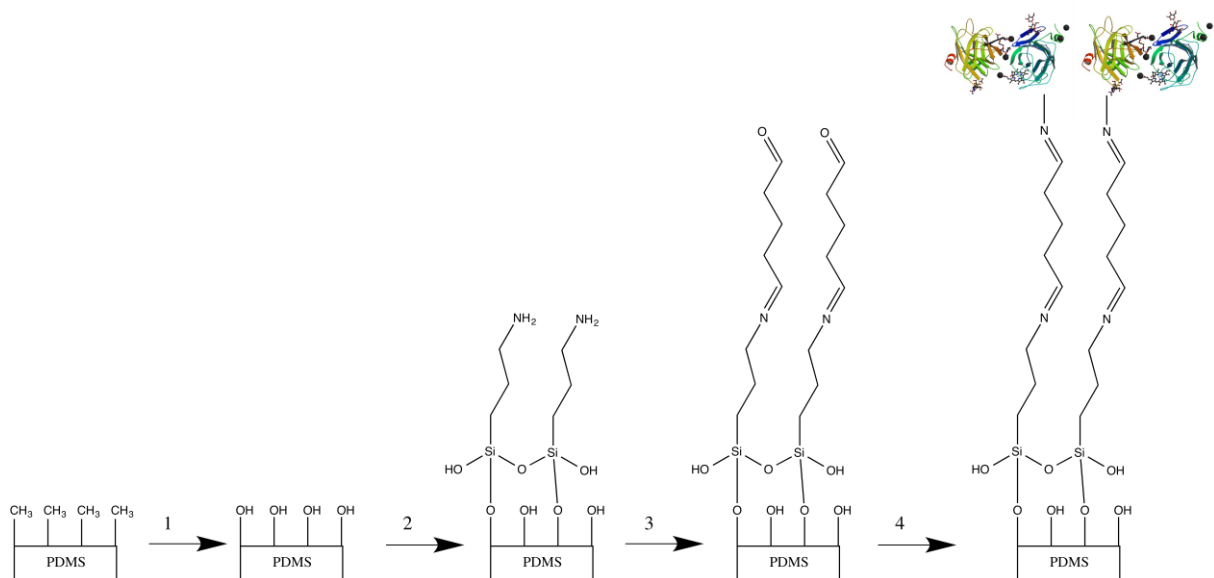


**Figure 13: Simplified immobilization reaction steps. 1) Activation of pdms 2) APTES silanization 3) Crosslinking with glutaraldehyde 4) CDH immobilization**

The purpose of the immobilization is to create an antibacterial catheter and hereby reduce the high infection rates of patients caused by biofilm formation on the surface of the catheter. The CDH does not only use the biofilm as a substrate but also produces hydrogen peroxide that is lethal to approaching bacteria.

## 1.3 Monitoring immobilization of CDH

### 1.3.1 Fourier transform infrared spectroscopy (FTIR)

FTIR is a spectroscopy method to maintain an infrared spectrum of adsorption, emission, photoconductivity or Raman scattering of a material in every state of matter (solid, gas, liquid). The raw data is transformed through Fourier transformation into the actual spectrum. The main advantage of a FTIR over a disperse spectrometer is that the FTIR collects spectral data in a wide range at the same time, compared to a narrower range of a disperse spectrometer[35].

A broadband light beam, that contains the full spectrum of wavelengths and shines into a Michelson interferometer, generates the wide range of spectral data. A Michelson interferometer consists of two mirrors - one moving, one static - and a beam splitter. The light from the polychromatic infrared source is adjusted to the beam splitter and there split, ideally 50/50 towards the moving and the static mirror. From there the splitted beams are reflected back and focused onto the sample and then to the detector. By moving the mirror, wavelengths are periodical blocked due to wave interference. Resulting from this effect different wavelengths are generated at different times which leads to different spectra each time. The light absorption for each mirror position has to be converted to a wavelength through the Fourier transformation to get the requested result. In Figure 14 a Michelson interferometer is shown[35].
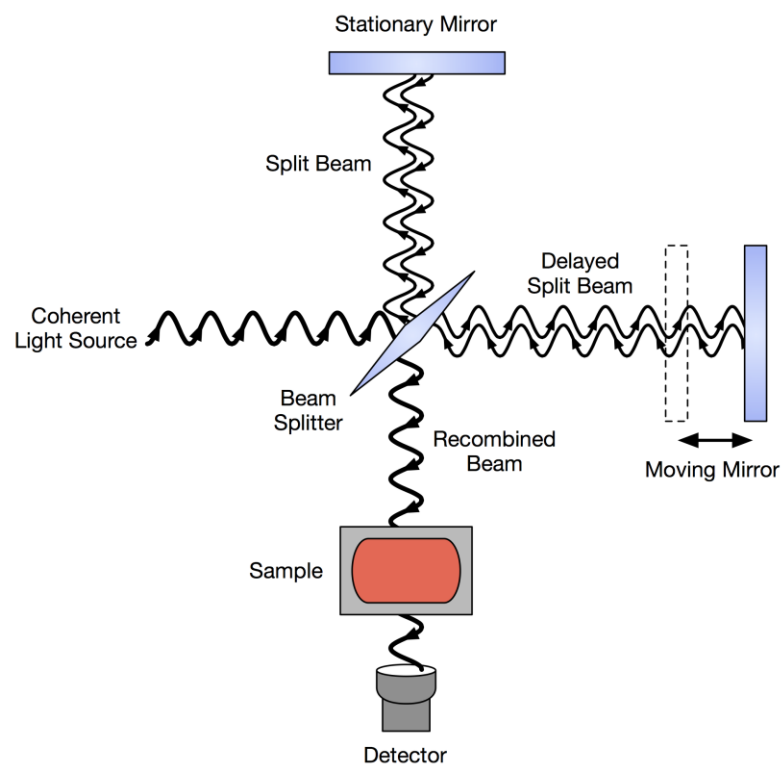


Figure 14: A Michelson interferometer consisting of 2 mirrors and a beam splitter

In this project a attenuated total reflectance (ATR) head was used to obtain spectra from solid samples. With this method solid samples can be analyzed without further preparation[36]. ATR uses a part of total internal reflection resulting an exponential decaying wave also called evanescent wave. A beam of infrared light is run through an ATR crystal that reflects at least once from the surface which is in contact with the sample, this reflection creates the evanescent wave and is then collected by a detector. With the wavelength, the angle of incidence, the indices of refraction, and the medium a result can be obtained[37]. In Figure 15 an ATR system is shown.
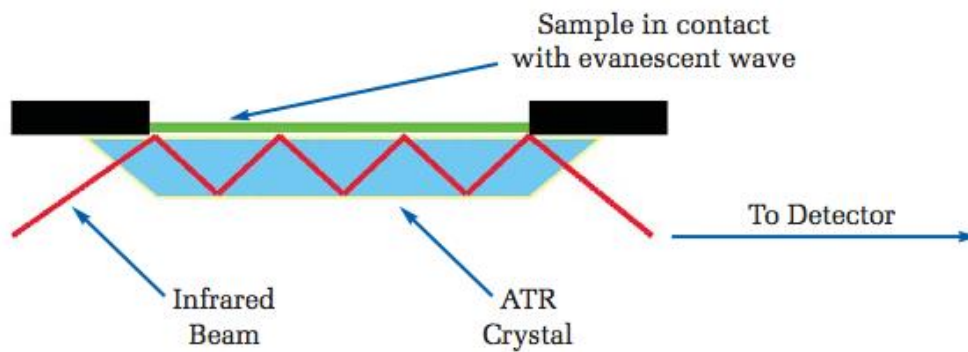


Figure 15: ATR system. A evanescent wave crosses the ATR crystal via reflection[36]

### 1.3.2   Water contact angle

The water contact angle provides information about the interaction of a liquid on a solid surface. It is also called wettability which corresponds to the hydrophilic or hydrophobic occurrence of a material. Is the water contact angle below 90° the surface is hydrophilic or has a high wettability, on the other hand if the water contact angle is above 90° the surface is hydrophobic and hast a low wettability[38]. In Figure 16 water drops on different surfaces are shown.
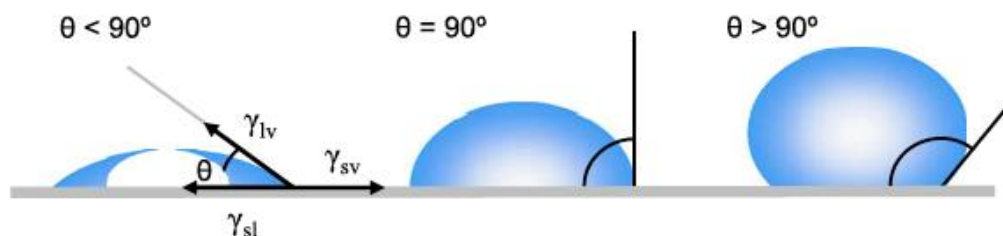


Figure 16: Water drops on different surfaces. < 90° a hydrophilic surface, > 90° a hydrophobic surface[38]

The shape of a liquid droplet on a surface depends on the surface tension of the liquid and the surface. In solution every molecule interacts equal with the neighboring molecule, resulting in a net force of zero.  But if molecules are exposed to a surface some neighbors are missing, and the

molecules are pulled inward, creating an internal pressure. The liquid droplet tries to keep up the lowest surface free energy, which means it interacts with the minimum needed surface area[38]. In Figure 17 these force in liquid droplet are shown.



**Figure 17: Interactions in a liquid droplet**[38]

### 1.3.3   Optical oxygen meter

The optical oxygen meter is used to determine the oxygen content in a solution. It is based on the luminescence radiation of luminophores. The luminophores get excited by red light and deliver the excitation energy to $O_2$ molecules, which results in a decrease of light emission in the infrared range. The signal decreases as the amount of oxygen increases. In Figure 18 and Figure 19 the mechanism of an optical oxygen meter is shown.
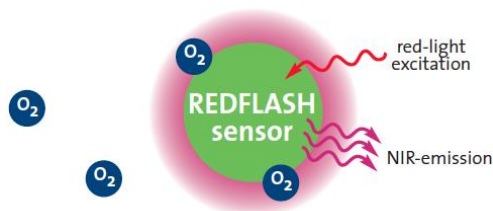


**Figure 18: Optical oxygen meter mechanism. The IR emission is high if there is a small amount of oxygen**
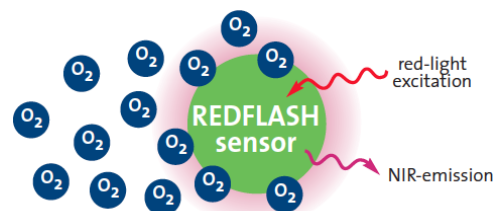


**Figure 19: Optical oxygen meter mechanism. The IR emission is low if there is a high amount of oxygen**

# 2  Material & Methods

## 2.1  CDH activity assay and immobilization studies

Throughout all experiments a modified cellobiose dehydrogenase  from *Myriococcum thermophilium* (MtCDH Oxyplus) developed by Roland Ludwig and Christoph Sygmund was used[39]. First the enzyme was characterized in regards to activity, protein concentration and $H_2O_2$ production. Different techniques were used.

### 2.1.1  2,6 dichlorophenolindophenol (DCIP)- CDH activity assay

The 2,6 dichlorophenolindophenol assay is used to measure the activity of cellobiose dehydrogenase. DCIP is a redox dye which is blue in its oxidized state (or red in acidic solutions) and colorless in its reduced state. In our case CDH oxidizes lactose and the electrons are transferred to DCIP which as a result is reduced. The reduction of absorbance is measured[40]. In Figure 20 the DCIP mechanism is shown.
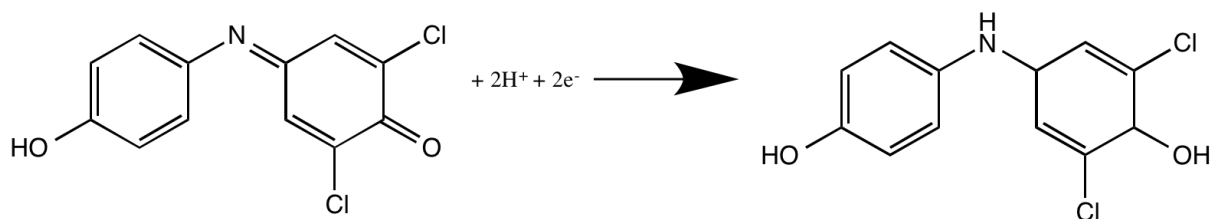


Figure 20: Reaction mechanism of 2,6 dichlorophenolindophenol

The assay was carried out as follows. The solutions that were used are shown Table 4.

Table 4: DCIP solutions

| Nr. | Solution | Concentration [mM] | Volume [µL] |
| --- | --- | --- | --- |
| 1 | DCIP solution | 3 (in 10% EtOH) | 100 |
| 2 | Lactose solution | 300 (in dest. Water) | 100 |
| 3 | Na-acetate buffer | 100, pH 4 | 780 |
| 4 | Sample (CDH) |  | 20 |

Solutions 1,2 and 3 were pipetted together and incubated  at 30°C for 20 min in a thermomixer. Then the sample was added and the reduction of absorbance was measured in a spectrophotometer at 520 nm. The activity was calculated with following equation and resulted in Unit/ml  [U/ml].

$$Enzyme\ factor\ EF = (cuvette\ volume * sample\ dilution\ factor)/(sample\ volume\ x\ \varepsilon)$$

$$Enzyme\ activity\ \left[\frac{U}{ml}\right] = EF * +slope$$

Table 5: Parameters for DCIP assay calculation

| Parameter | Value |
|---|---|
| Cuvette volume | 1 [ml] |
| Sample dilution factor | 0 |
| Sample volume | 0,02 [ml] |
| $\varepsilon_{520nm}$ | 6,9 [mM$^{-1}$ cm$^{-1}$] |

For a temperature profile of the CDH the solutions 1,2 an 3 were heated up to 30°C, 40°C, 50°C, 60°C, 70°C, 80°C, 90°Cand 99°C and the sample was added and measurement started immediately

### 2.1.2 Monitoring oxygen consumption during incubation of CDH with Cellobiose – optical oxygen meter

As the CDH reduces $O_2$ to $H_2O_2$, the oxygen consumptions is another method to determine the activity of the enzyme. The solutions shown in Table 6 were submitted.

Table 6: Solutions for optical oxygen meter

| Nr. | Solution | Concentration [mM] | Volume [μL] |
|---|---|---|---|
| 1 | Na-acetat buffer | 100 | 1000 |
| 2 | Lactose in dest. water | 300 | 200 |

To start the reaction 200 μL of CDH were added and the oxygen consumption was recorded over night. For a pH stability test of the CDH, buffers with different pH values (4, 5, 6, 7, 8, 9, 10, 11) were used.

## 2.1.3  Monitoring the hydrogen peroxide production of CDH - Amplex® red assay

The amplex red assay is used to determine the $H_2O_2$ production of CDH. CDH oxidizes the substrate (cellobiose) and transfers the electrons to $O_2$ which results in the reduction to $H_2O_2$. The amplex red reagent reacts with $H_2O_2$ in a 1:1 stoichiometry and produces the red-fluorescent resofurin with help of a horseradish peroxidase. The mechanism is shown in Figure 21.
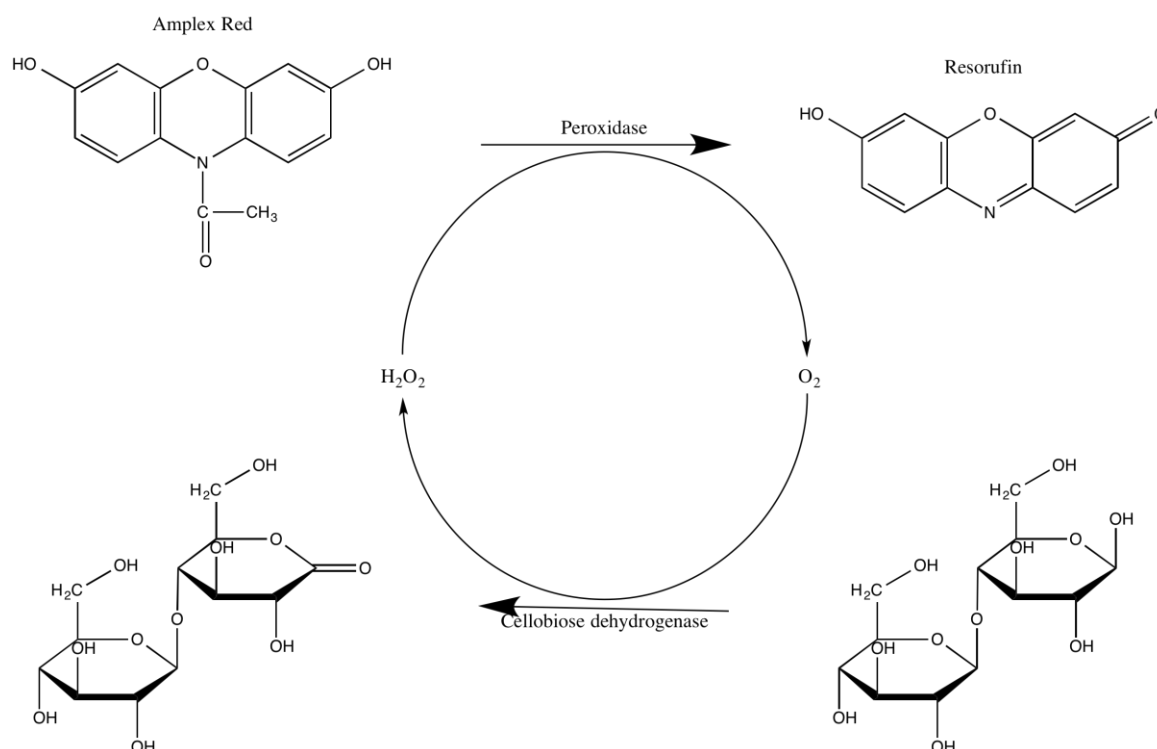


Figure 21: Amplex red assay mechanism

The reaction was carried out in 96-well plate with following solutions shown in Table 7.

Table 7: Solutions for amplex red assay

| Nr | Solution | Stock solution concentration | Concentration in assay | Volume in 96-well (200 [µL]) |
|----|----------|------------------------------|------------------------|------------------------------|
| 1 | Amplex red | 10 [mM] | 25 [µM] | 0,5 [µL] |
| 2 | Peroxidase | | 0.1 [U/ml] | 2 [µL] |
| 3 | Cellobiose | 200 [mM] | 30 [mM] | 30 [µL] |
| 4 | CDH | | | 10 [µL] |
| 5 | NaPO$_4$ buffer | 0.25 M pH 7.4 | | 157.5 [µL] |

Solutions 1,2,3 and 5 were pipetted together, and the reaction was started with the addition of the CDH. Resofurin has an excitation maximum at 550 nm and an emission maximum at 587 nm. The reaction was monitored on a platereader. The used settings are shown in Table 8.

Table 8: Plate reader settings for amplex red assay

| Paramenter | Value |
|---|---|
| Kinetic cycles | 30-120 |
| Interval time | 00:01:00 |
| Mode | Top reading |
| Excitation wavelength | 550 nm |
| Emission wavelengh | 587 nm |
| Excitation bandwidth | 9 nm |
| Emission bandwidth | 20 nm |
| Gain | 73 |
| Number of reads | 5 |

The amplex red assay was also used to determine the $H_2O_2$ production of the immobilized CDH on silicone. For this purpose 425 µL of the 0,25M $NaPO_4$ buffer, 75 µL of the 200mM cellobiose and the immobilized CDH on silicone were put into an eppendorf tube and incubated for 3h for the layer by layer technique and 5 minutes for the covalent immobilization method at 40°C and 600 rpm. 197,5 µL were transferred a into a 96-well plate, then 0,5 µL of amplex red and 2 µL of peroxidase were added to start the reaction.

### 2.1.4 Protein content determination - the bicinchoninic acid (BCA) assay

In this study BCA was used to monitor the silicone immobilized or residual CDH in solution. The BCA assay is used to determine the total protein concentration in a solution. The color change of the solution from green to purple is proportional to the protein concentration in the sample.

The BCA solution contains bicinchoninic acid, $Na_2CO_3$, $NaHCO_3$, sodium tartrate and cupric sulfate pentahydrate. The assay relies on two reactions: first the peptide bonds of the protein reduce $Cu^{2+}$ ions from the cupric sulfate to $Cu^+$, then two molecules of the bicinchoninic chelate with each $Cu^+$ ion and form a purple colored product, which absorbs light at 562 nm. The amount of $Cu^{2+}$ reduced is proportional to the amount of protein in the solution.

The BCA assay was carried out in a 96-well plate as follows. First a BCA working solution was prepared as shown in Table 9.

Table 9: BCA working solution

| BCA solution | 200 µL |
|---|---|
| 4% cupric sulfate | 4 µL |

200 µL of the BCA working solution were mixed with 25 µL sample, then mixed for 30 seconds and incubated at 37°C for 30 min. After the plate cooled down to room temperature it was measured at 562 nm. Every sample was measured in duplicates or triplicates

### 2.1.5    Protein content determination - Roti nanoquant assay

The estimated of bound and unbound CDH were further analyzed using the Roti nanoquant technique. Another determination method for the protein concentration is the Roti nanoquant assay. It is a modification of the bradford assay. The reaction mechanism is based on complex building with cationic and nonpolar side chains of the protein. The dye Coomassie Brilliant Blue G-250 has an adsorption shift from 470 nm in its unlinked state to 595 nm in its bound state. The assay was carried out exactly as described the instruction for use[41]. Every sample was measured in duplicates or triplicates.

### 2.1.6    Protein content determination – Nanodrop method

The nanodrop method was the third method used for the determination of the protein concentration. It uses the advantage that aromatic side chains of proteins have their absorption maximum at 280nm. The settings for the method are shown in Table 10.

Table 10: Settings for the Nanodrop protein content measurement

| Sample drop volume | 2 µL |
|---|---|
| Molecular weight of CDH | 88 kDA |
| Extinction coefficient of CDH | 159000 |

Before the measurement the detector head was cleaned with 2µL ddH$_2$O. Of every sample a triple determination was made.

## 2.2 Sample preparation

### 2.2.1 PDMS samples

Catheters and silicone were kindly provided by DEGANIA SILICONE LTD Israel. For all following experiments silicone was sliced into 1 cm x 1 cm pieces or stamped out into round pieces with a diameter of 6 mm to fit into 96-well plates shown as in Figure 22 and Figure 23. Before every experiment those plates were washed with approx. 70% EtOH.



Figure 22: 1cm x 1 x cm silicone plates



Figure 23: round silicone plates with a diameter of 6 mm

### 2.2.2 Fluorescein isothiocyanate (FITC) labelling

For fluorescent labeling of CDH the dye FITC was used. FITC was dissolved in anhydrous dimethylsuloxid (DMSO) at a concentration of 1mg/ml. Solutions containing 1mg/ml, 2mg/ml and 5mg/ml of CDH in 0,1 M Carbonat pH 9 buffer were used. To these solutions a 5 fold excess of FITC compared to the molecular weight of CDH in solution was added and incubated over night at 25°C. The unbound protein was then separated via size exclusion chromatography on a so-called AEKTA purifier with the parameters shown in Table 11.

Table 11: AEKTA purifier settings

| Column | 5ml desalting column |
|---|---|
| Flow rate | 1ml/min- 3ml/min |
| Sample loop | 2ml |
| Fraction size | 500 µl |
| Mobile Phase | Needed buffer |

If the protein concentration was too low after the purifying process, vivaspins were used to concentrate the sample.

## 2.3 Enzyme immobilization

### 2.3.1 Layer by Layer technique

The 1x1 cm silicone pieces were dipped into following solutions alternately. 3 different approaches were performed as shown in Figure 24.
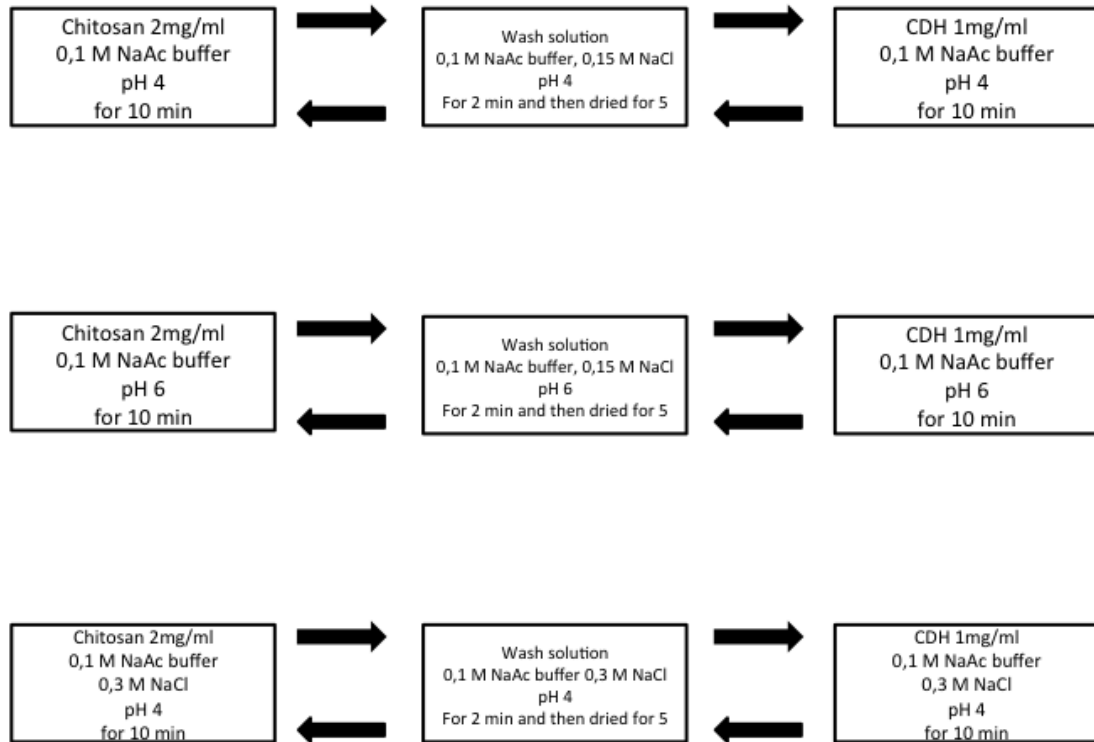


Figure 24: Layer by layer experimental scheme

One dipping cycle yields one bilayer, 6 cycles were performed and analyzed using FTIR and the DCIP assay. Also a FITC labeled enzyme was used.

### 2.3.2 PDMS activation

**Piranha solution**

98% H2SO4 was provided and then 35% $H_2O_2$ was slowly added. The ratio between the 2 solutions was 3:2. Silicone plates were incubated in it over night at room temperature under constant stirring. On the next day the treated silicone plates were put in to a 1M KOH solution for 1h, to provide more –OH groups. The activated silicone plates were analyzed for changes in the water contact angle. Of every sample a triple determination was made and the average of the right and left angle of the drop were taken.

**Plasma gas discharge**

The plasma machine was from Diener Plasma surface technology with a generator frequency performance of 13,56 Mhz which was stage less adjustable from 0% - 100%. As a gas oxygen was used. The silicone samples were put into the machine and a vacuum was created for 3 min. The plasma charge settings that were used are shown in Table 12.

Table 12: Plasma machine settings

| Time [min] | Frequency | $O_2$ Sscm (standard cubic centimeters per minute) |
|---|---|---|
| 2, 5 | 100% | 15, 20 |

The changes on the surface were analyzed by measuring the water contact angle at different time points after the plasma process.

After the treatment the plates were inserted into the APTES solution.

### 2.3.3 Silanization using APTES

For the APTES silanization the following solution was prepared: 1 ml APTES + 5 ml 0.1M Acetic Acid (99%) + 5ml isopropanol. To hydroxylate the silanes and create linkages between them, the solution was mixed for 2h. Then the silicone plates were transferred into this solution and incubated over night (24h) under steady mixing at 30 rpm on a rotator After the incubation step, the APTES treated silicone plates were incubated at 100°C for 1h to remove the water as shown in Figure 11.

**Ninhydrin test - Amine group detection**

To prove that there are amine groups present on the surface the APTES treated plates were dipped into, or sprayed with a 2% Ninhydrin solution. Afterwards the samples were heated at 100°C until a color change was visible.

### 2.3.4 Glutaraldehyde mediated grafting of CDH

Immediately after the APTES treatment the silicone plates were put into a glutaraldehyde solution. Subsequent solutions were used as shown in Table 13.

Table 13: Glutaraldehyde conditions

| % of Glutaraldehyde (w/w) | Buffer |
|---|---|
| 0.5% | 0.1 M NaPO$_4$ pH 7.3 |
| 5% | 0.1 M NaPO$_4$ pH 7.3 |
| 10% | 0.1 M NaPO$_4$ pH 7.3 |
|  | 0.05 M citrate pH 5.5 |
|  | 0.1 M KPO$_4$ pH 6 |
|  | 0.1 M NaPO$_4$ pH 8 |

The silicone plates were left in the glutaraldehyde solution and mixed for 10 min at 30 rpm on a rotator. To create a hydrolytically stable secondary amine the silicone plates were put into a 2.5M NaCNBH$_3$-solution for 10 min. Afterwards the silicone plates were washed 2 times with buffer and 1 time with dH$_2$O.

### 2.3.5 Enzyme immobilization

The CDH immobilization step was carried out in buffer solutions shown in Table 14 over night under constant stirring.

Table 14: Buffers used for enzyme immobilization

| Buffer |
|---|
| 0.05 M Citrate pH 5.5 |
| 0.1 M KPO$_4$ pH 5.5 |
| 0.1 M NaPO$_4$ pH 7.3 |
| 0.1 M NaPO$_4$ pH 8 |

Enzyme concentrations and immobilization conditions were varied as shown in Table 15.

Table 15: CDH immobilization conditions. For example CDH 0.5 mg/ml was immobilized at 25° and 4° with no addition but also at 25° and 4° with 10 mM cellobiose.

| CDH concentration [mg/ml] | Temperature [°C] | Add on |
|---|---|---|
| 0.5 | 4 | No  or 10 mM cellobiose |
| 1 | 25 |  |
| 3 | 25 |  |
| 7 | 4 | No or 10 mM cellobiose |

1 mg/ml was used for immobilization with different glutaraldehyde concentration, 3 mg/ml was used for determining the optimal pH value, 0,5 mg/ml and 7mg/ml were used for optimizing the immobilization conditions.

After the immobilization the silicone plates were washed 2 times with buffer and one time with dH$_2$O. To analyze the samples FTIR and the amplex red assay were used. When FITC labeled CDH was used for the immobilization process the silicone sheets were analyzed concerning their fluorescence using the BIO RAD Chemidoc. All samples were stored at 4°C.

## 2.4 Analysis

### 2.4.1 Monitoring surface modification using FTIR technique

All measurements were performed on a FTIR spectrometer Perkin Elmer 100 with 4 scans per spectrum and a resolution of 4 cm$^{-1}$. Before the FTIR measurement the ATR-head was cleaned with approx. 70% EtOH. The samples were inserted on the crystal and pressure applied to obtain a clear spectrum. All spectrs were normalized at the highest peak at 785 cm$^{-1}$ which stands for the Si-C stretching of PDMS, and should not be modified by layer by layer technique or plasma treatment.

### 2.4.2 Measuring surface activation of modified PDMS using water contact angle measurement

The water contact angle measurement was performed with following settings shown in Table 16

Table 16: Water contact angle measurement settings

| Parameter | Value |
|---|---|
| Drop | mQ - water |
| Volume rate | 405,1 |
| Volume | 3 µl |
| Zoom | 8 |
| Focus | 5 |

On every sample 8 drops were measured. The highest and the lowest value were deleted, and the average value of the rest was taken for determination.

### 2.4.3 Zeta potential measurement

The SurPASS measurement was realized by Mühlbacher Inge of the polymer competence center Leoben. Following measurement conditions were used:

- Measurement solution: high purity water, 1 mM KCl, pH value: 6.3
- Maximum applied pressure: 300 mbar, titration with 0.05 M HCL
- Evaluation of zetapotential: Helmholtz -  Scholuchowski
- Determination of the isoelectric point (IEP)
- After each measurement the SurPass was cleaned to avoid a procrastination of CDH or CS.

Following samples were measured: One layer CDH, one layer Chitosan,CDH-CS 1 and CS-CDH 2.

# 3   Results & Discussion

## 3.1   Preliminary characterization of cellobiose dehydrogenase

After receiving the enzyme, characterization experiments were performed in order to find the perfect conditions for the immobilization process. The DCIP assay was performed in triplicates to obtain the enzyme activity. The negative slopes of the decreasing of absorbance are shown in Table 17.

Table 17: Slopes of DCIP assay

| Slope | Average |
|---|---|
| -1.368 | |
| -1.308 | -1.304 |
| -1.236 | |

To calculate the activity Equation 3 and Equation 4 were used.

The Enzyme factor is 7.25 which results in an enzyme activity of **9.45 U/ml** multiplied with the average of the measured slopes.

There was also temperature profile of CDH recorded at different °C shown in Table 18.

Table 18: Results for temperature profile of CDH

| T [°C] | k | U/ml |
|---|---|---|
| 30 | 0.599 | 4.3 |
| 40 | 0.767 | 5.6 |
| 50 | 1.07 | 7.8 |
| 60 | 1.291 | 9.4 |
| 70 | 1.271 | 9.2 |
| 80 | 1.367 | 9.9 |
| 90 | 0.61 | 4.4 |
| 99 | 0.179 | 1.3 |
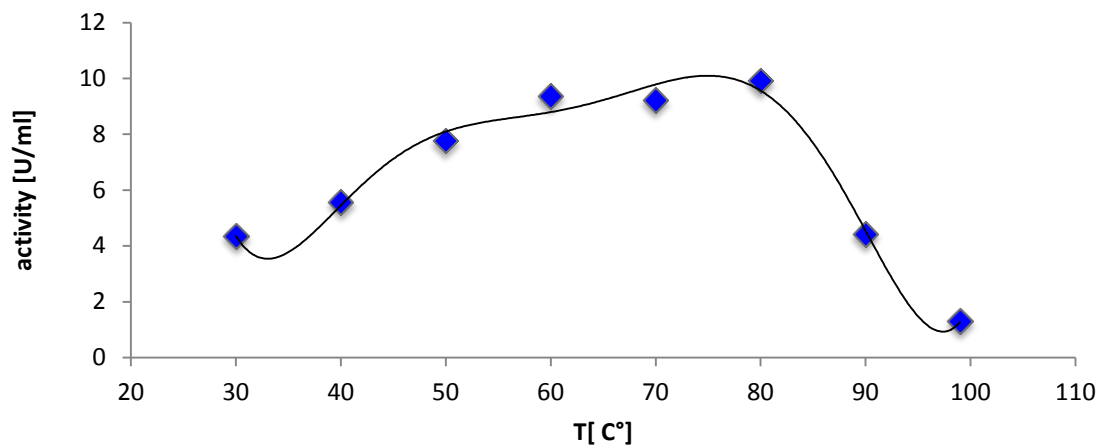
The temperature profile proves that the enzyme derives of a thermophile organism (*Myriococcum thermophilium)*, the highest activity value is at 80 °C. The activity difference between activity measured above and the activity from the T-profile at 30° (9.45 U/ml) is because the enzyme used for the temperature profile comes from another fermentation batch.

### 3.1.1 pH profile

As the DCIP dye isn't stable against pH changes, the pH profile was measured using the oxygen optical meter. The decrease of oxygen in solution is measured as shown in Figure 25.
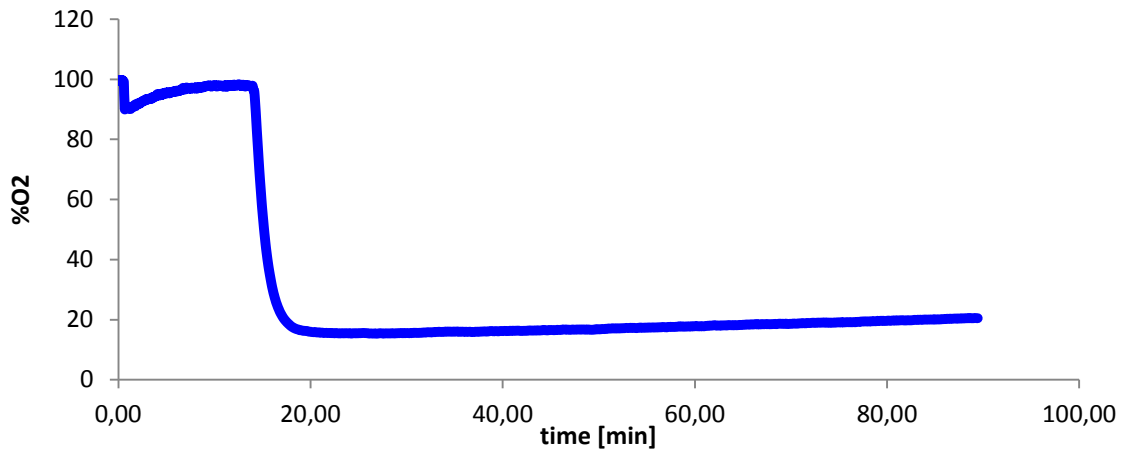


**Figure 25: Decrease of oxygen measured with a optical oxygen meter at pH 4**

The highest value before the addition of the enzyme was taken as the 100% oxygen reference. All values were normalized using this reference in order to yield oxygen curves that all start at the same point. The decrease of oxygen was monitored over time and the slope with the unit % oxygen consumption of the enzyme per minute is shown in Figure 26.



$$y = -45,13x + 736,96$$
$$R^2 = 0,99$$
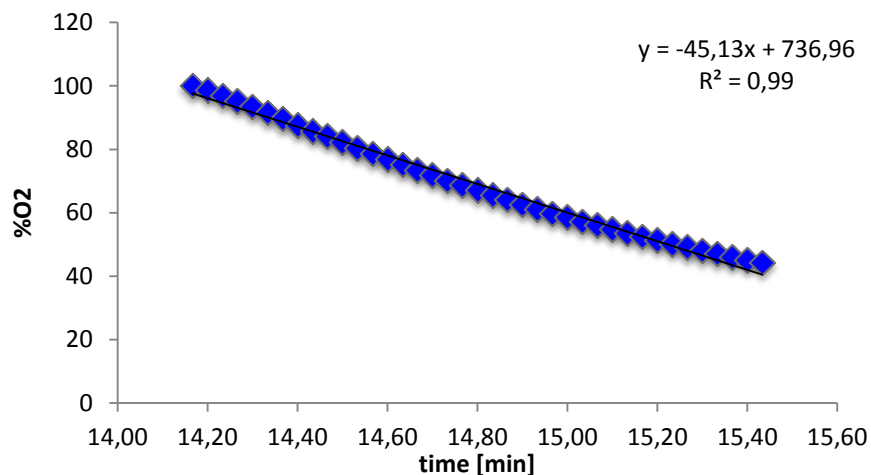
**Figure 26: Normalized oxygen consumption at pH 4**

For the pH values 5,6,7,8,10,11 the oxygen consumption was measured the same way and the results are shown in the appendix. The results are shown in Table 19 and Figure 27.

**Table 19: Oxygen consumption of CDH at different pH values**

| pH | [$\%O_2$/min] |
|----|------------|
| 4  | 45.13 |
| 5  | 31.81 |
| 6  | 53.32 |
| 7  | 51.21 |
| 8  | 57.07 |
| 10 | 55.17 |
| 11 | 31.16 |
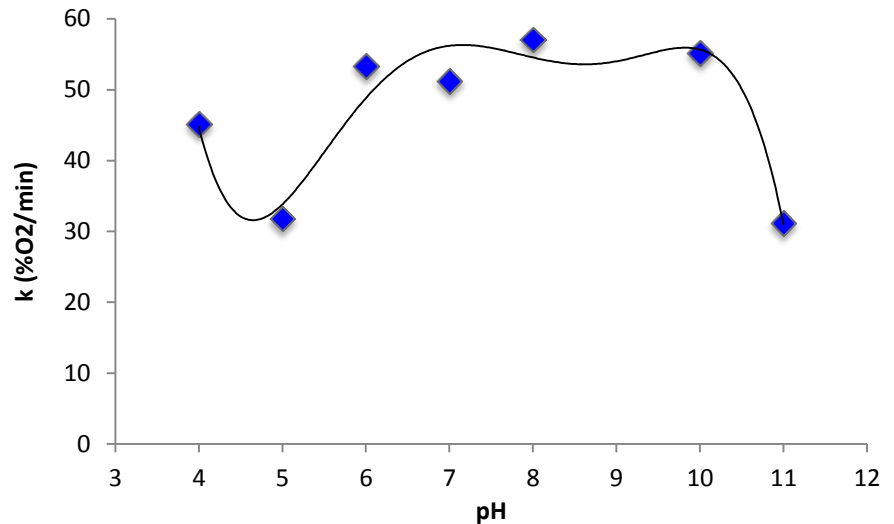


Figure 27: Oxygen consumption of CDH at different pH values

The highest oxygen consumption of the enzyme was at pH 8, the lowest activity was at pH 5.

### 3.1.2 Amplex red assay

Another way to determine the activity of CDH was the $H_2O_2$ production.

A calibration curve with fixed $H_2O_2$ values was produced and is shown in Table 20 and Figure 28

**Table 20: Amplex red assay calibration curve values**

| $H_2O_2$ [µM]. | Emission |
|-----------|----------|
| 0    | 5495.4 |
| 2.3  | 13052.4 |
| 4.6  | 20022.5 |
| 10.4 | 27411.7 |
| 15.1 | 31971.7 |



$$y = 1671.9x + 8757.1$$
$$R^2 = 0.93565$$
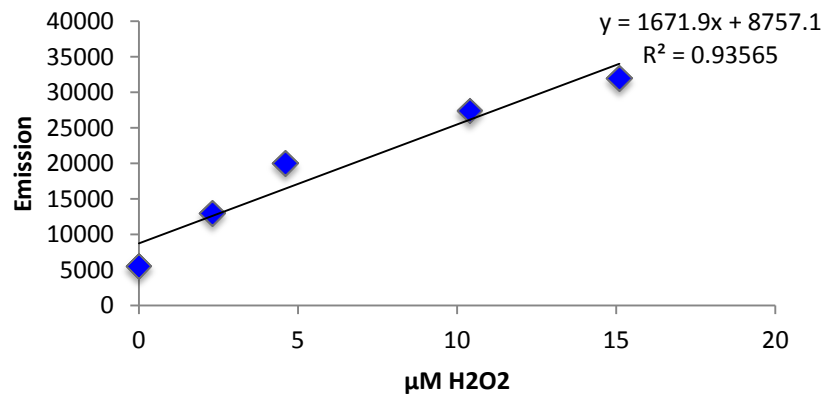
Figure 28: Amplex red assay calibration curve

With the equation 1671,9x + 8757,1 the $H_2O_2$ production of the enzyme was calculated. The emission curve of the fluorescent signal of the enzyme is shown in Figure 29. The sample was 1:100 diluted.
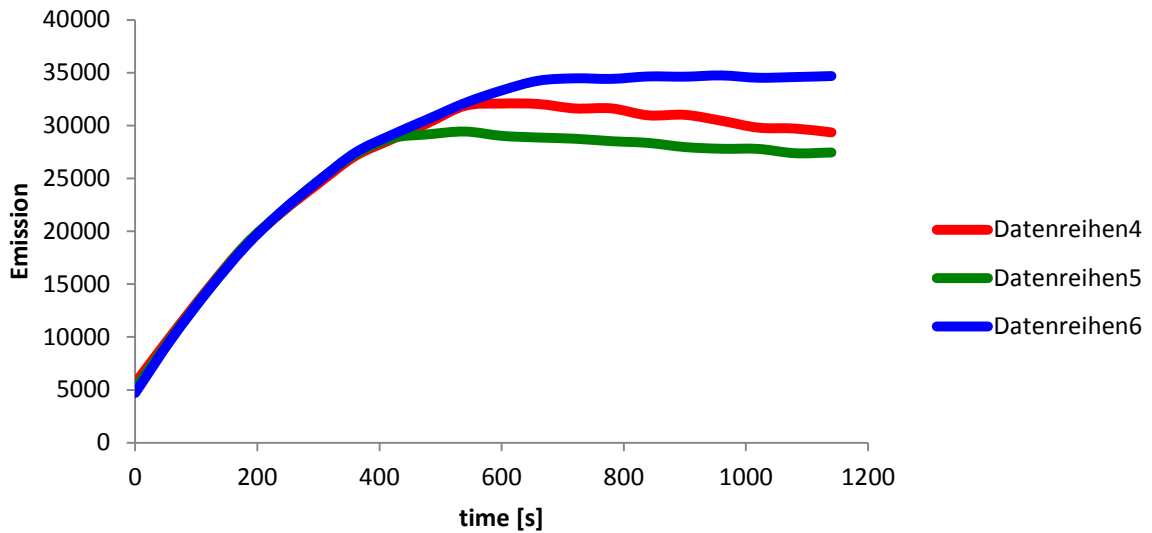
Figure 29: Amplex red fluorescent emission spectra for CDH

Series 4,5 and 6 are produced from the same sample. The average value of the curves from 600 to 1000 sec was used to calculate the $H_2O_2$ production and is shown in Table 21.

Table 21: Results of $H_2O_2$ determination of CDH

| Time [min] | Emission | $H_2O_2$ [µM] (1:100) | $H_2O_2$ [µM] | $H_2O_2$ [mM] |
|---|---|---|---|---|
| 5 | 24682 | 9.5 | 953 | 1 |
| 10 | 30635 | 13.1 | 1308 | 1.3 |

After 5 min of incubation the enzyme produced **1 mM** of $H_2O_2$ after 10 min **1.3 mM**.

The signal reaches a steady state after 600 seconds (10 min). That the signal is constant at this point could be caused by some reasons. It is assumed that the curve should rise linear, as the enzyme produces $H_2O_2$ until the substrate or the dye is consumed. There is the possibility that CDH gets inhibited by a high concentration of its product $H_2O_2$. As in nature the electron acceptor is not $O_2$ it is possible. Another reason would be that detector was no able to differentiate the high fluorescent signal of the solution.

The data for the production after 5 min will be used as comparisons to the immobilized enzyme.

### 3.1.3  BCA assay

To calculate the protein concentration a BCA assay was performed. First a calibration curve with following values shown in Table 22 was created.

| BSA [µg/ml] | E (Abs) |
|---|---|
| 1000 | 1.541 |
| 500 | 0.8955 |
| 250 | 0.54245 |
| 125 | 0.3215 |
| 25 | 0.1386 |
| 0 | 0.0989 |

Table 22: BCA calibration curve values
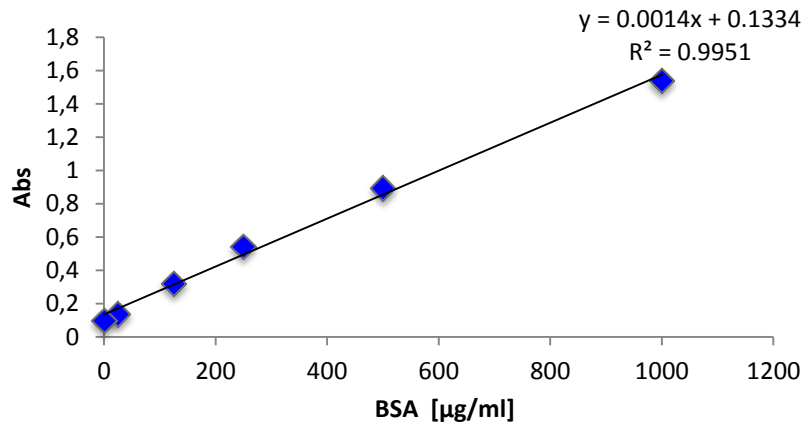


Figure 30: BCA calibration curve

With the equation y = 0.0014x + 0.1334 the protein concentration was calculated. As the first measurement was out of the calibration area, the sample was diluted 1:100.

The final protein concentration was **23.5 mg/ml.**

### 3.1.4 Roti nanoquant assay

The second assay for the determination of the protein concentration was the Roti nanoquant assay. The quotient results of OD590/OD450 of Human Serum Albumin (HSA) for the calibration curve are shown in Table 23 and the calibration curve Figure 31.

| Table 23: Values for Roti Nanoquant calibration curve | |
|---|---|
| HSA [µg/ml] | OD 590 / OD450 |
| 1 | 0.5461 |
| 2.5 | 0.5498 |
| 5 | 0.5624 |
| 10 | 0.6415 |
| 25 | 0.8166 |
| 50 | 1.1600 |
| 75 | 1.4705 |
| 100 | 1.9279 |
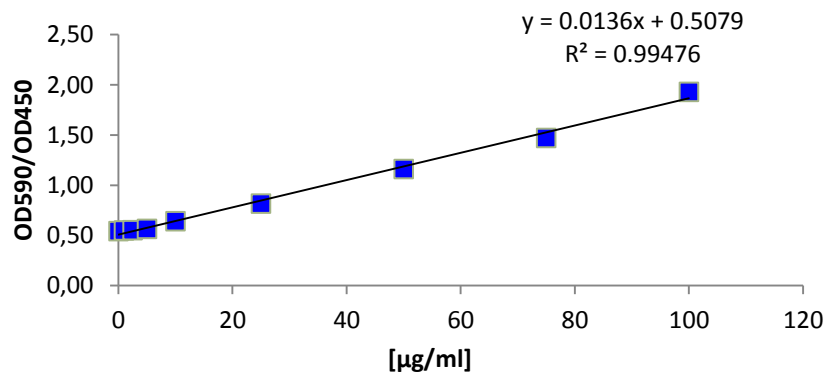


Figure 31: Roti Nanoquant calibration curve

The quotient of CDH was 2.94, which was used in the equation $y = 0.0136x + 0.5079$ resulted in a protein concentration of **17.8 mg/ml.**

### 3.1.5 Nanodrop method

The third protein concentration determination method was using the nanodrop which resulted in following concentrations shown in Table 24.

| Table 24: Nanodrop protein concentration results | |
|---|---|
| Concentration [mg/ml] | Average [mg/ml] |
| 10.01 | |
| 9.72 | 9.83 |
| 9.76 | |

The protein concentration was **9.83 mg/ml.**

The activity measurement of CDH shows that the enzyme derives from a thermophile organism, with its highest activity at 80°C. Also CDH likes a broad pH range, from slightly acidic to moderately basic (pH 6 to pH 10). The comparison of the activity of the DCIP assay and the optical oxygen meter is difficult, as the enzyme is genetically optimized to transfer the electrons faster to oxygen than to other acceptors, in case of the DCIP assay to dichlorphenolinophenol.

The different calculations for the overall protein concentration points out that the assays react with different functional groups of the protein. The BCA assay shows the highest concentration, which

was predictable because of its reaction mechanism. All amino acids are cross-linked via peptide bonds that produce the signal for the BCA assay. The difference between the other 2 assays indicates that there are more nonpolar and cationic amino acids (Roti nanoquant) in the protein than amino acids with aromatic side chains (Nanodrop). For further experiments the value **23.5 [mg/ml]** was used**.**

In Table 25 all results for CDH are summarized.

Table 25: Summary of results of enzyme characterization

| Assay | CDH [mg/ml] | Specific activity [U/mg] | $H_2O_2$ production [µmol/mg protein] |
|---|---|---|---|
| BCA | 23.5 | 0.4 | 110 |
| Roti Nanoquant | 17.8 | 0.5 | 146 |
| Nanodrop | 9.8 | 0.9 | 265 |

## 3.2 Enzyme immobilization

### 3.2.1 Layer by Layer technique

The fact that PDMS is uncharged on the surface made it difficult to predict if charged molecules would interact with the surface. Because of the positive inductive effect of –CH3 (+i) it was expected that there should be a slightly positive charge on the surface, which meant that the first layer should be negatively charged to interact with the surface. The isoelectric point of CDH is 3.9, which meant that the pH of the enzyme solution should be above this value in order to reach a negative net charge of the enzyme. Another limitation was the solubility of chitosan which is only soluble in solution with a pH under 6.4. The layer by layer technique was performed at pH 4 and 6.

**FTIR analysis of PDMS samples after layer by layer treatment**

- *pH 4 CDH as first layer*

In Figure 32 the spectrum of PDMS after the layer by layer treatment at pH 4 with CDH as the first layer is shown.



CDH – CS 1    CDH – CS 5
CDH – CS 2    CDH – CS 6
CDH – CS 3    Reference
CDH – CS 4
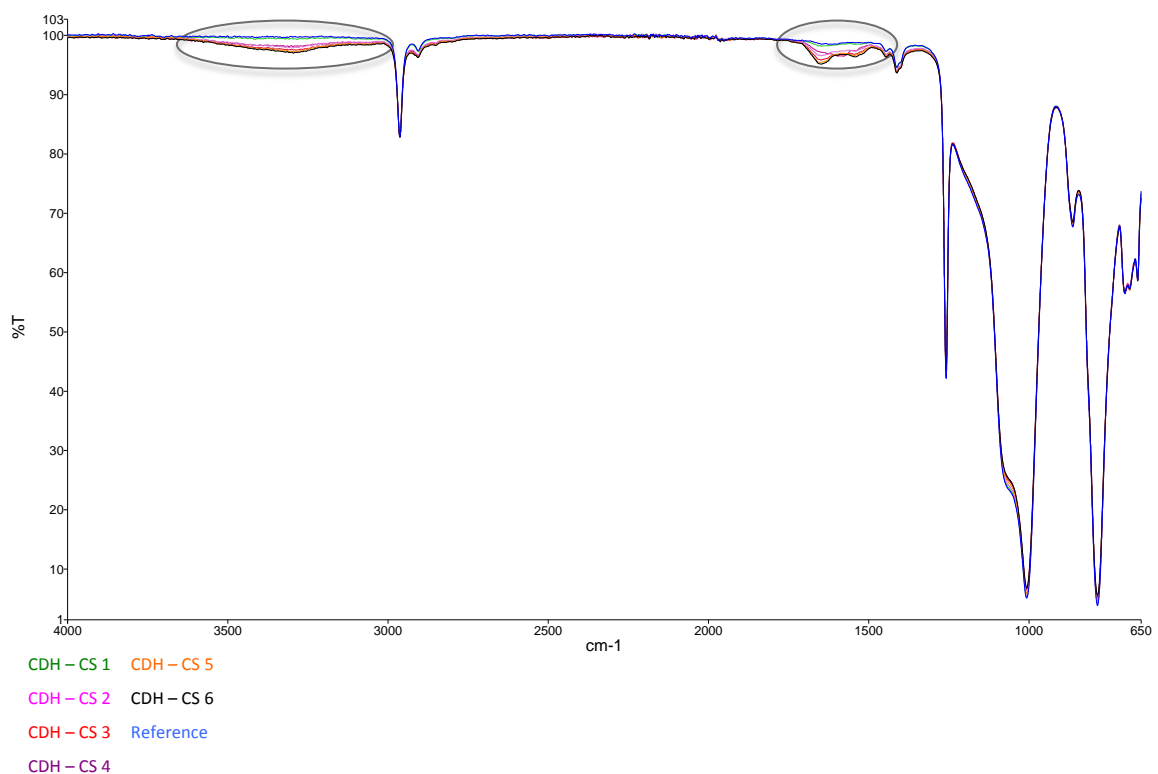
**Figure 32: FTIR spectrum of PDMS treated with Layer by layer method at pH 4 and CDH as the first layer. The number after CDH-CS stands for the number of bilayers for example CDH-CS 2 means 2 bilayers.**

There is a clear difference between the spectra of the layer by layer treated plates compared to the reference (untreated silicone plate, blue line) at wavenumber 3600 - 3200 $cm^{-1}$ and 1700 - 1400 $cm^{-1}$ marked by black circles. The broad band at 3600 - 3200 $cm^{-1}$ is representative for an –OH group in a

hydrogen bond. Hydrogen bonds are very typical for protein interactions that occur between amides. They are also are a big factor in defining the 3D structure of proteins. In Figure 33 and Figure 34 the FTIR band and hydrogen bonds between amino acids are shown.



CDH – CS 1  CDH – CS 3  CDH – CS 5  Reference
CDH – CS 2  CDH – CS 4  CDH – CS 6
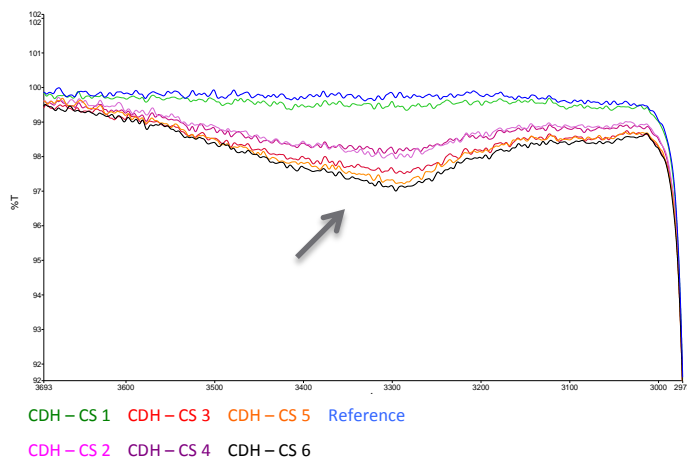
Figure 33: FTIR peak of hydrogen bond peaks of proteins after layer by layer treatment at pH 4
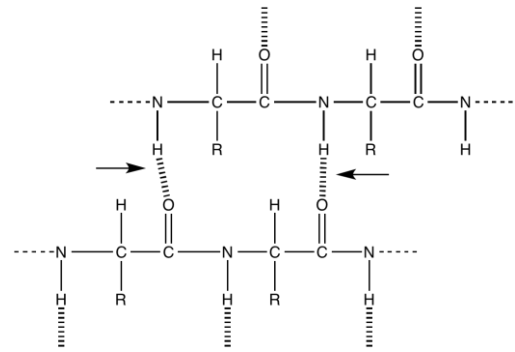


Figure 34: Hydrogen bonds between amides of amino acids

The second difference between the reference (blue line) and the layer by layer treated plates occurs at 1700 - 1400 cm$^{-1}$. Technically speaking there are two main peaks, one at 1690 - 1640 cm$^{-1}$ and the other one at 1640 - 1550 cm$^{-1}$. Those two peaks are typical for amide bonds. The peak at 1690 - 1640 cm$^{-1}$ stands for the N-H bending vibration and the peak at 1640 - 1550cm$^{-1}$ for the C=O stretch vibration of an amide bond. The vibrations and the FTIR peaks of amides are shown in Figure 35 and Figure 36.



CDH – CS 1  CDH – CS 3  CDH – CS 5  Reference
CDH – CS 2  CDH – CS 4  CDH – CS 6
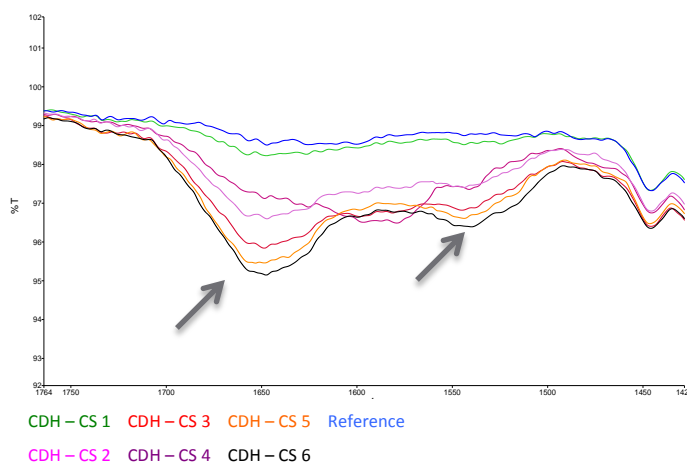
Figure 35: FTIR peaks of amide bonds after layer by layer treatment at pH 4
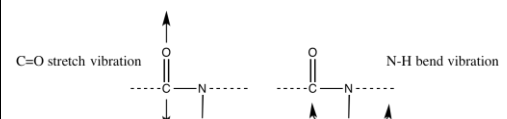


Figure 36: Amide bond vibrations

The FTIR spectra show no system behind the intensity of the peaks corresponding to the different number of layers (3 layers show a higher intensity than 4). This will be discussed later in this chapter after more results are known.

The spectra of the samples with chitosan as the first layer are shown in the appendix.

- *pH 4 + 300 mM NaCl*

NaCl was added to increase the ionic strength, and change the conformation of CDH to enable better binding properties. CDH was used as the first layer. The FTIR spectrum is shown in Figure 37.



CDH – CS 1    CDH – CS 4    Reference

CDH – CS 2    CDH – CS 5

CDH – CS 3    CDH – CS 6
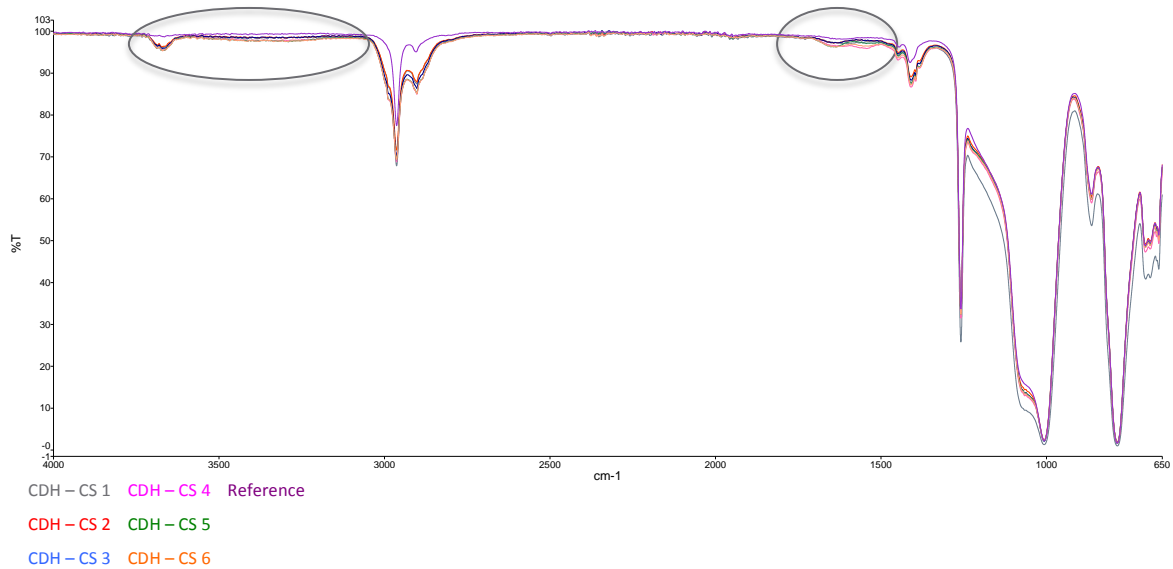
**Figure 37: FTIR Spectrum of PDMS treated via layer by layer technique at pH 4 with 300mM NaCl**



CDH – CS 1    CDH – CS 3    CDH – CS 5    Reference

CDH – CS 2    CDH – CS 4    CDH – CS 6
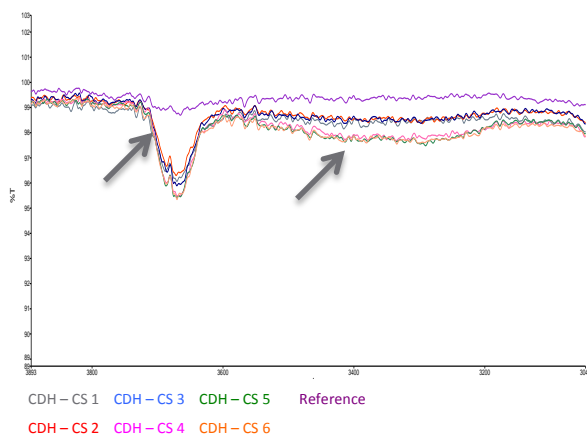
**Figure 38: -OH FTIR peaks of PDMS samples treated with layer by layer method at pH 4 with 300 mM NaCl**



CDH – CS 1    CDH – CS 3    CDH – CS 5    Reference

CDH – CS 2    CDH – CS 4    CDH – CS 6
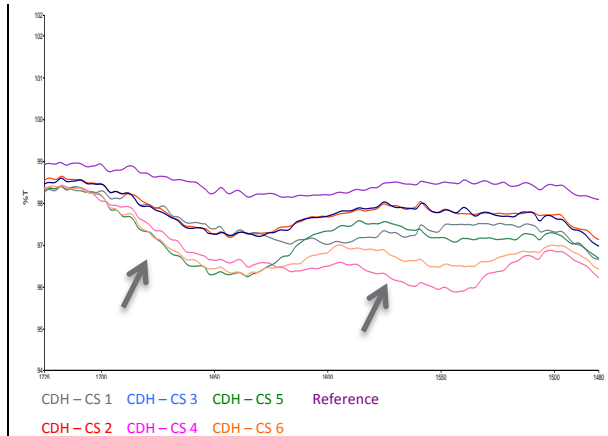
**Figure 39: FTIR spectrum of amide bonds of PDMS treated with layer by layer technique at pH 4 with 300mM NaCl**

Compared to the spectrum of the samples treated without 300mM NaCl there is a clear difference at the peak at 3670 cm$^{-1}$ shown in Figure 38. The band is not as broad as expected for –OH group in a hydrogen bond. It is sharp which is typical for –OH groups that are not bonded. The exact correlation to the higher ionic strength is unclear but a possible explanation is that the positive charge of sodium interferes with hydrogen of the amide to build up a hydrogen bond. There is also a broad peak visible

at 3600 - 3200cm$^{-1}$ but its intensity is very small compared to the spectrum shown in Figure 33. The two peaks for amide bonds in Figure 39 are also small and not clearly visible.

- *pH 6*

In Figure 40 the FTIR spectrum of PDMS treated with layer by layer technique at pH 6 is shown. CDH is again the first layer. Black circles mark the areas for the hydrogen bonds and the amide bonds of proteins. In Figure 41 and Figure 42 they are shown in more detail.



| Name | Beschreibung |
| --- | --- |
| CDH – CS 1 | CDH – CS 4 |
| CDH – CS 2 | CDH – CS 5 |
| CDH – CS 3 | Reference |
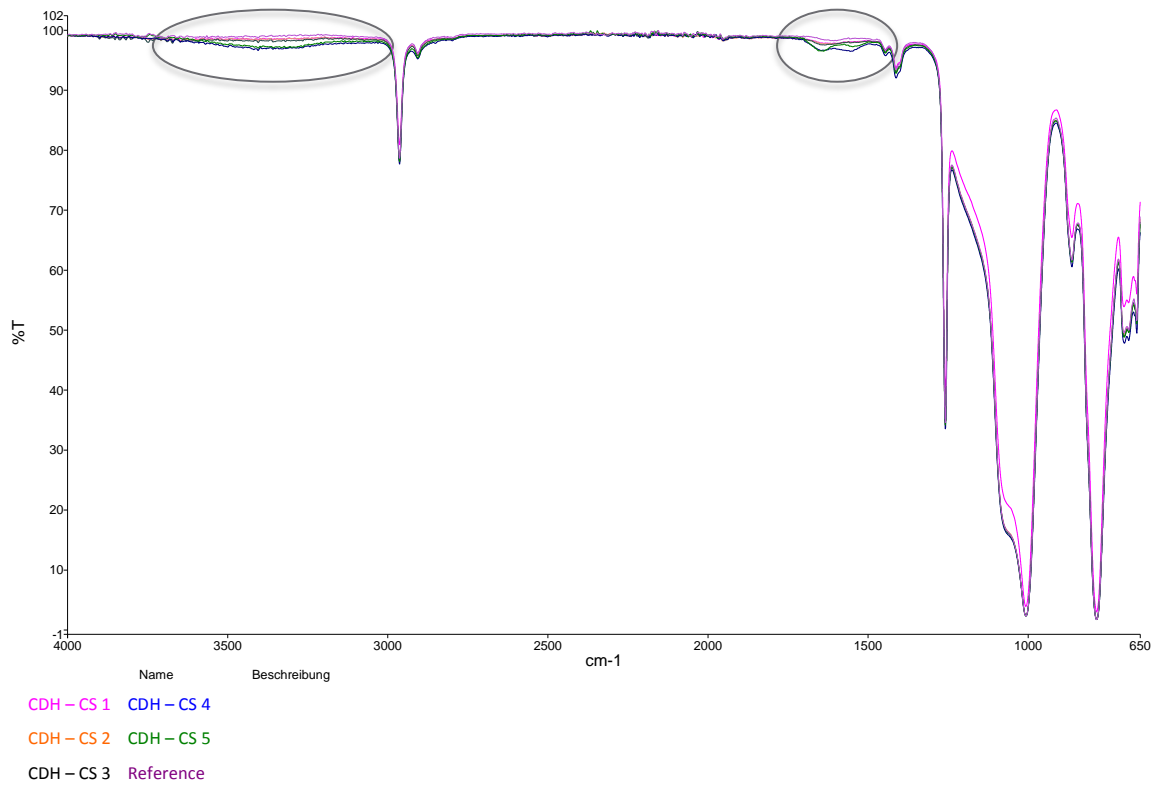
**Figure 40: FTIR spectrum of PDMS treated with layer by layer method at pH 6 with CDH as the first layer**



| CDH – CS 1 | CDH – CS 3 | CDH – CS 5 |
| --- | --- | --- |
| CDH – CS 2 | CDH – CS 4 | Reference |
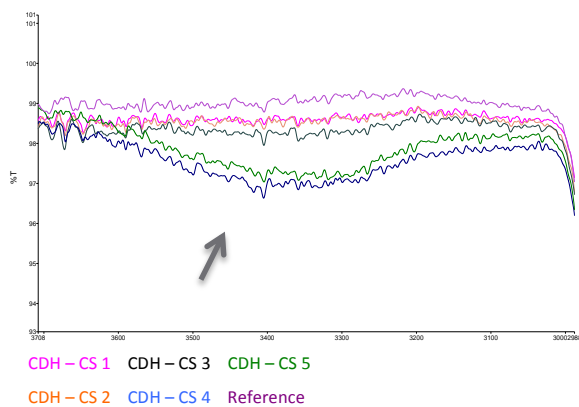
**Figure 41: FTIR peak of hydrogen bonds at pH 6**

| CDH – CS 1 | CDH – CS 3 | CDH – CS 5 |
| --- | --- | --- |
| CDH – CS 2 | CDH – CS 4 | Reference |
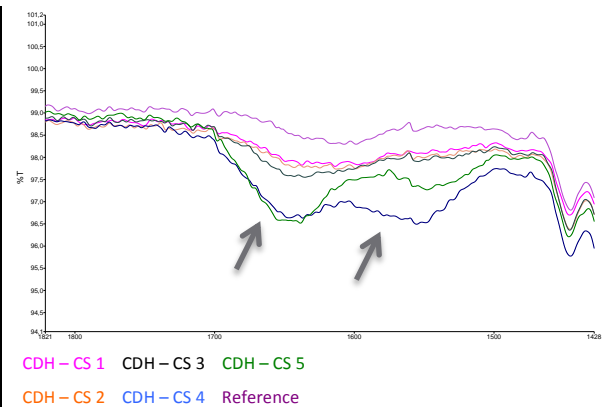
**Figure 42: FTIR peaks of amide bonds at pH 6**

The spectrum in Figure 40 from the PDMS samples treated via layer by layer technique at pH 6 compared to the one treated at pH 4 shown in Figure 33, show less intensity of the important peaks, which concludes that less CDH interacts with the surface. Again there is no system visible referred to the number of different layers. The blue line that stands for 4 layers has a higher intensity than the green line, which stands for 5 layers. The FTIR spectra with Chitosan as first layer are shown in the appendix.

**Detection of the enzyme activity of the immobilized enzyme**

To prove that the enzyme is bound to the PDMS surface and active a DCIP assay of the silicone plates treated at pH 4 was performed. Unfortunately it was difficult to measure the activity with a silicone plate in the cuvette because it interferes with the light beam of the spectrophotometer. No useful activity was measured. The samples were left in cuvettes over night to see if the color of the DCIP changes after a longer period of time. The result is shown in Figure 43.
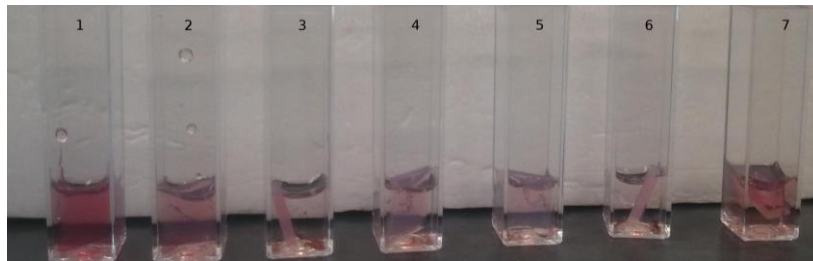


**Figure 43: DCIP result of PDMS samples treated via layer by layer technique at pH 4, incubated over night**

The cuvette with number 1 is the negative control, cuvettes with numbers 2-7 are the treated samples ordered by increasing number of layers (2 is one bilayer, 7 is 6 bilayers). There is a slight color change recognized between the samples. The sample with 5 layers (nr. 6) is clearer than the one with 1 layer (nr. 2). The sample 7 with 6 bilayers was cut into two pieces to fit into the cuvette, the darker color of the solution is a result of the smaller overall surface of the sample compared to the other samples. The two pieces were put really close together. This test shows that there is some reaction going on and the enzyme is active but very slow.

The samples treated at pH 6 and pH 4 with 300 mM didn't show any activity.

**Hydrogen peroxide production capacity of immobilized enzyme**

The amplex red assay was performed to see if CDH produces $H_2O_2$ after the layer by layer treatment. Due to material and equipment limitations of all the treated silicone plates, just 3 spot tests were analyzed. The incubation time was 3h and the reference is a negative control (silicone only). The description for example LbL – CDH-CS – pH 4 -1 means: Layer by layer – CDH as the first layer at pH 4 and 1 for 1 bilayer. In Table 26 and Figure 44 the results are shown.

Table 26: $H_2O_2$ production of CDH on PDMS after layer by layer treatment

| Sample | $H_2O_2$ [µM] |
|---|---|
| Reference | 1.7 |
| LbL - CDH-CS - pH 4 - 1 | 3.8 |
| LbL - CDH-CS - pH 4 - 3 | 9.1 |
| LbL - CDH-CS - pH 4 - 6 | 9.6 |
| LbL - CDH-CS - pH 4 - 300mM NaCl - 1 | 3.9 |
| LbL - CDH-CS - pH 4 - 300mM NaCl - 4 | 11.8 |
| LbL - CDH-CS - pH 4 - 300mM NaCl - 6 | 14.4 |
| LbL - CDH-CS - pH 6 - 2 | 9.9 |
| LbL - CDH-CS - pH 6 - 3 | 13.2 |
| LbL - CDH-CS - pH 6 - 5 | 12.7 |
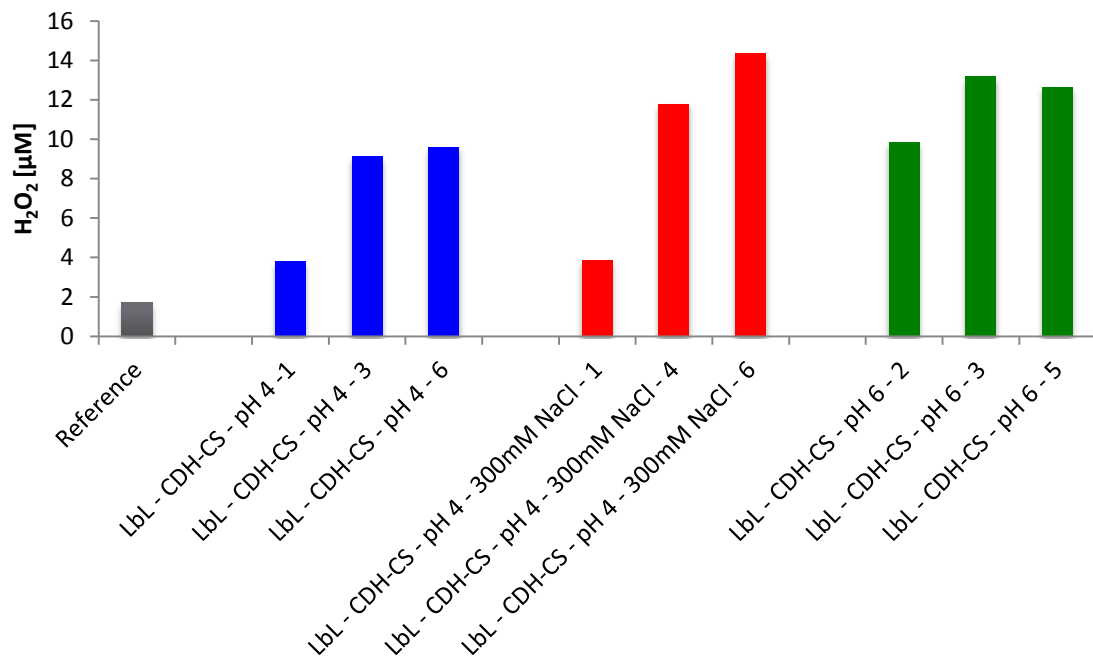


Figure 44: $H_2O_2$ production of CDH on PDMS samples after layer by layer treatment

The $H_2O_2$ production of CDH at pH 4 with and without NaCl correlates with the increasing number of bilayers. The highest production of $H_2O_2$ after 3h happened at 6 bilayers at pH4 with 300 mM NaCl with a value of **14.4 µM**. There is also at good production at pH 6, but there is no system visible that correlates with the bilayer number. The results for the $H_2O_2$ production do not correlate with the

results of the FTIR measurement. An explanation is that the FTIR measurement only analyzes one exact point of the treated PDMS sample, but the layer distribution can differ on the whole surfaces. Another point is that the FTIR spectra are all spectra of transmission. As transmission is defined by the intensity of the radiation coming out of the sample divided by the intensity of radiation shining into the sample, there is no possibility to quantify the result and compare them with actual values.

**Surface charge analysis - Surpass Measurement**

The First measurement served as control if the Surpass machine was clean  a polypropylene sheet which has its isoelectric point at pH 4, was used. The measurement is shown in Figure 45.
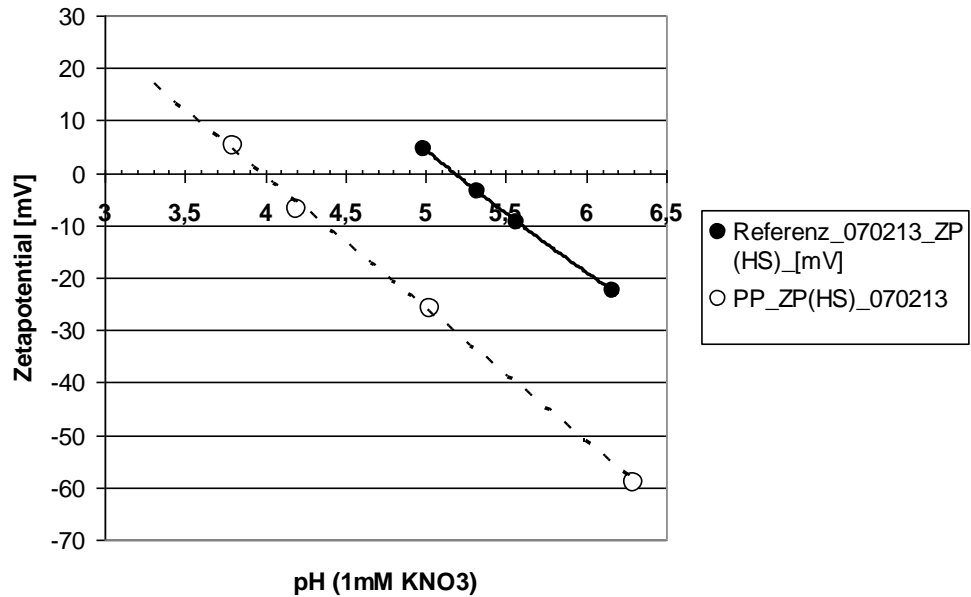


Figure 45: Control for cleanness of the Surpass machine

The result for the measurement of just CDH and CS is shown in Figure 46.
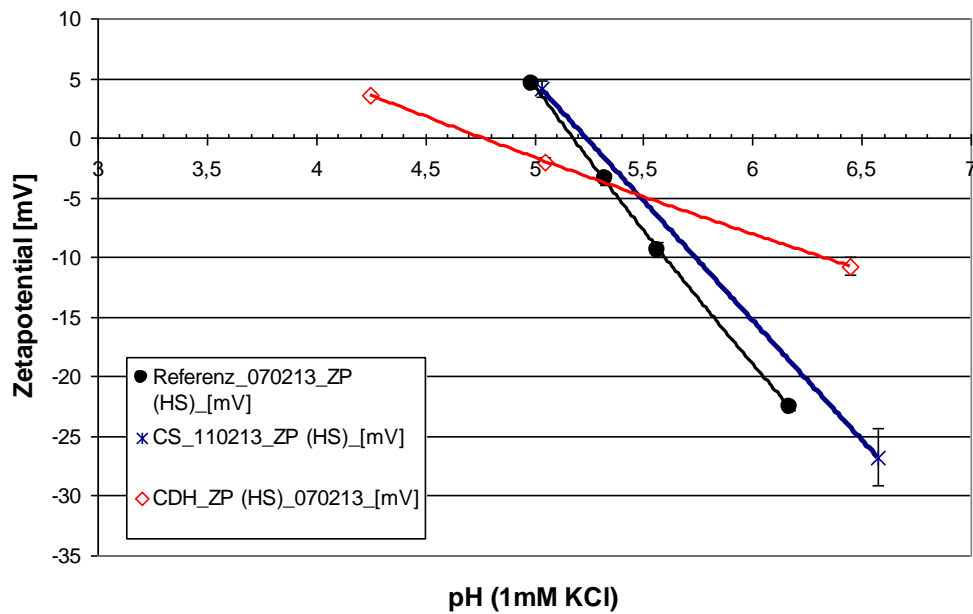


Figure 46: Zetapotentail measurement of CDH or CS

CS_110213_ZP (HS)_[mV] stands for the samples which was treated with just chitosan. CDH_ZP (HS)_070213_[mV] stands for the sample treated with just CDH.

CDH (red line) shifts the IEP in acidic direction, which concludes that it adsorbs to the PDMS surface, in contrast CS does not adsorb to the surface and therefore no shift of the IEP can be seen.

In Figure 47 the results from all zetapotential measurements are shown.
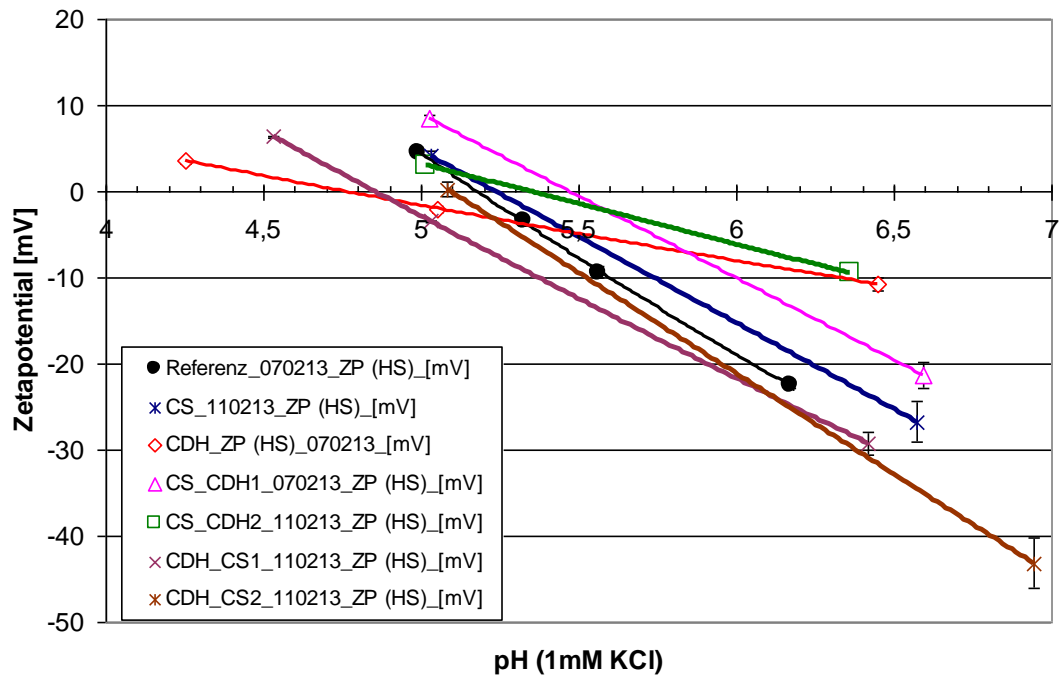


Figure 47: Summary of Zetapotential measurements

CS_CDH1 stands for one bilayer with chitosan as its first layer, CS-CDH2 for 2 bilayers. CDH-CS1 means CDH is the first layer of one bilayer, CDH-CS2 stands for 2 bilayers.

Following conclusions of the zetapotential measurement were made.

- The IEP of PDMS is displaced compared to other inert surfaces (polypropylen, polyethylene terephthalate, poly(methyl methacrylate). A possiblie explanation is a contamination due to the manufacturing process.
- Chitosan does not adsorb to the surface.
- CDH does adsorb to the surface.

All samples have a negative charge in a neutral pH area.

The results in this section show that the Layer by layer technique worked. There are clear indications in the FTIR spectra that CDH interacted with the surface of PDMS. As mentioned above the spectra are spectra of transmission and it is not possible to compare the results of the different layering conditions with the help of spectra. On the other hand the amplex red assay proves that CDH is active and attached to the surface of PDMS. The highest production of $H_2O_2$ was reached at pH 4 with 300mM NaCl after 6 layering cycles. There is also a trend visible in increased $H_2O_2$ production resulting from the increasing number of layers. It is unclear if layer built up is achieved by CDH and chitosan bilayer. Chitosan does not adsorb to PDMS referring to the surpass measurement. It could also be possible that Chitosan does not adsorb to CDH, and the increasing $H_2O_2$ production with increasing number of layers resulted due to the longer time the enzyme was exposed to PDMS through more cycles of layering. The layer by layer technique with chitosan is also found in literature, the main difference is that chitosan interacts with a hydrophilic surface which PDMS clearly does not [42]. The fact that Chitosan does not adsorb to PDMS was also the reason why FTIR spectra with Chitosan as the first layer were moved to the appendix, as they look the same as the ones with CDH as the first layer.

### 3.2.2 Activation of PDMS for immobilization of CDH

**PDMS surface activation via piranha solution**

After 24h incubation in $H_2O_2/H_2SO_4$ and 1h in 0.1M KOH the PDMS samples were brittle and lost their transparency. It was visible to the naked eye that the piranha solution attacked the surface as it was not flat anymore which made the analysis of the roughed up surface was difficult.

The water contact angles are shown in Table 27 and Figure 48. The number 1,2 and 3 stand for 3 samples treated with the same piranha solution.

Table 27: Water contact angles of piranha treated PDMS

| Sample | Average water contact angle |
|---|---|
| Reference | 105.6° ± 6.2° |
| 1 | 102.9° ± 7.3° |
| 2 | 105.4° ± 4.6° |
| 3 | 101.1° ± 7.9° |
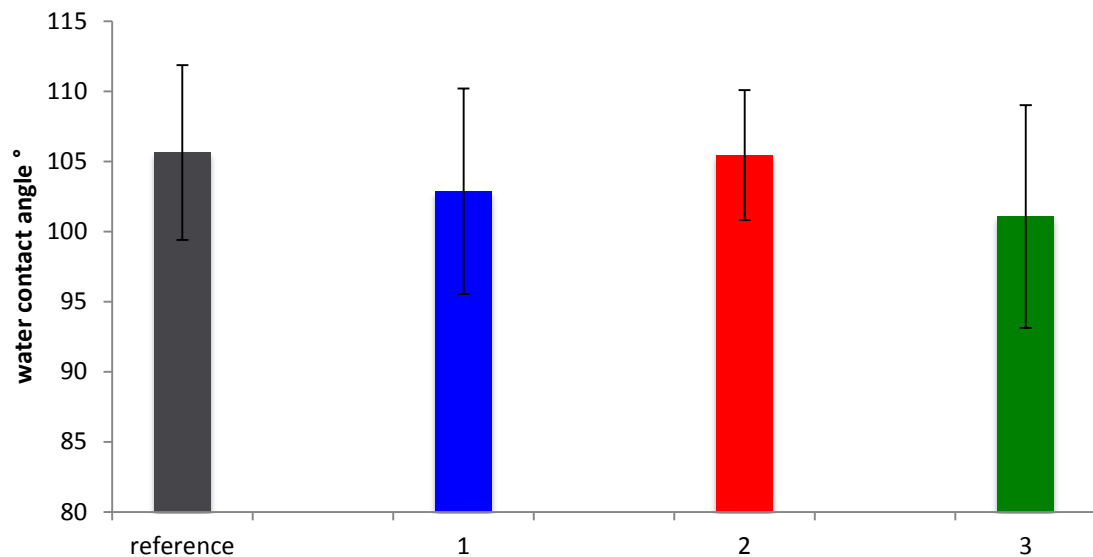


Figure 48: Water contact angles of piranha treated PDMS

There was no change in the water contact angle. Due to the rough surface it was difficult to place drops that were stable. The FTIR measurement confirmed the results that there was no change of funktional groups on the surface. The FTIR spectrum is shown in Figure 49.
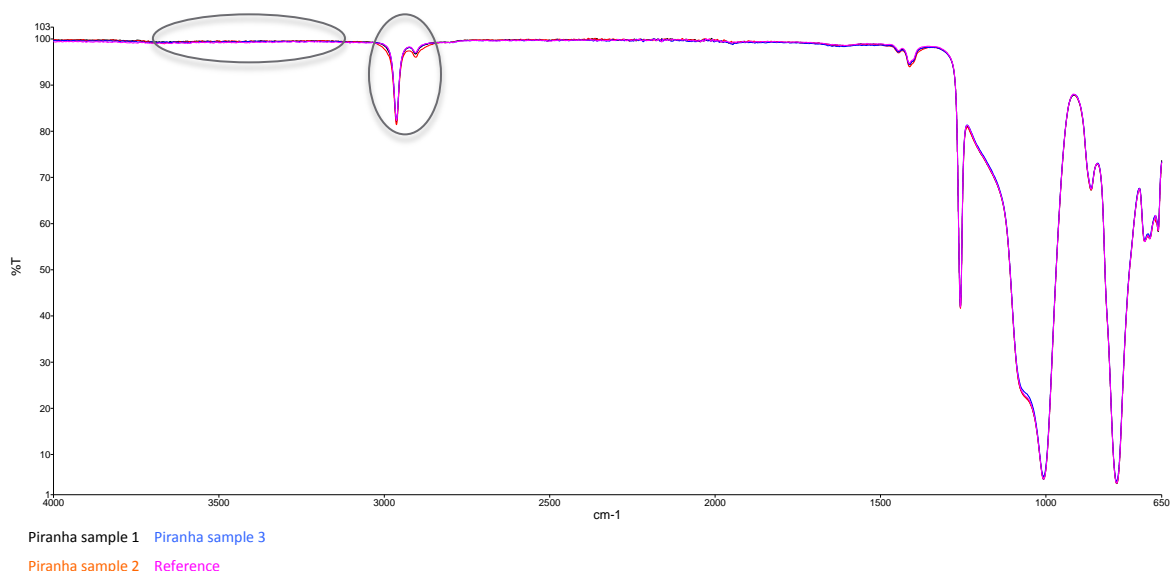
**Figure 49: FTIR spectrum of piranha treated PDMS**

There should be a change visible at the areas marked in black. Between 3600 - 3200cm$^{-1}$ there should be a peak for the introduced –OH bonds and the sharp peak at 3000 - 2800cm$^{-1}$, which is the -CH$_3$ vibration, should be decreased. None of these changes happened.

The introduction of –OH groups onto the surface of PDMS via piranha solution did not work. Both analyzing measurements (WCA and FTIR) of all 3 samples showed no difference compared to the untreated sample. The inert molecular structure of PDMS could be the reason for these findings. In a 3D structure the bonds of a polymer are really strong and hard to attack even by the highly oxidative piranha solution. The visible change of the surface could be caused by depletion, but there was no change in the chemical structure. As the activation did not work, it was senseless to continue with further immobilization steps. In Literature this method worked for very thin PDMS films, the water contact angle decreased after 5 min of piranha solution treatment from ≈109° to ≈65° and after 30 minutes to ≈30° [43]. Though the structure of these thin PDMS films is very different to the PDMS samples used in this work. The probes used in this work are defined by a 2 mm thick and highly stable 3D network, which appears to be vary hard to attack.

**PDMS surface activation by plasma treatment**

To prove that the surface activation worked, water contact angles were measured. The measurement was performed immediately, 15 min and 30 min after the plasma process. Settings for the first plasma process were: **100% frequency, 15 sccm of $O_2$ for 2 and 5 minutes**. Water contact angles are illustrated in Table 28 and Figure 50.

Table 28: Water contact angles after plasma process with 100% and 15sccm of $O_2$

| Time [min] | 0 | 15 | 30 |
|---|---|---|---|
| reference | 103.9° ± 5.3 | | |
| 2min exposed to plasma gas | 37.4° ± 6.3° | 45.2° ± 7.9° | 67.8° ± 10.0° |
| 5min exposed to plasma gas | 31.3° ± 7.2° | 58.5° ± 11.5° | 70.1° ± 7.7° |
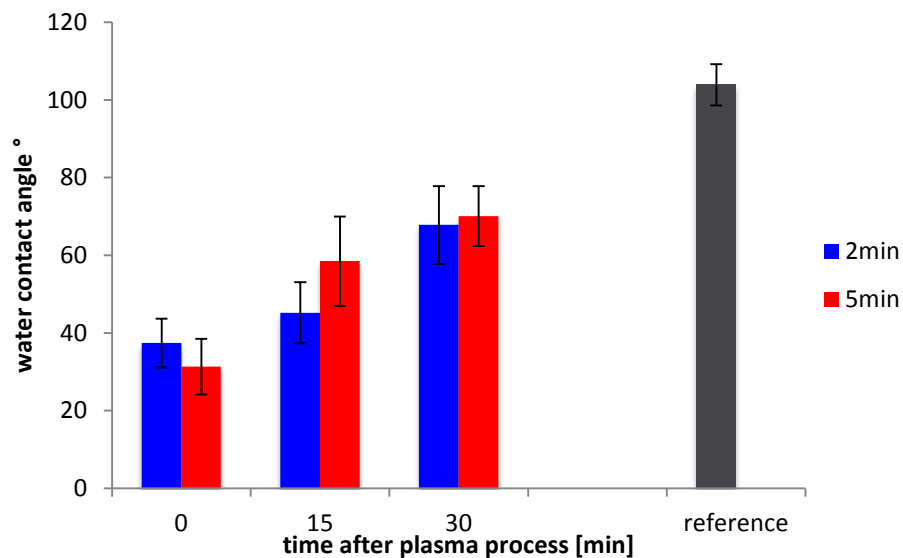


Figure 50: Water contact angles after plasma process with 100% and 15 sccm of $O_2$

It is clearly visible that the plasma process changes the occurrence of the PDMS surface. The decreasing water contact angle derives from the introduction of –OH groups and the resulting increased hydrophilicity. Exposing time of PDMS to plasma gas does not change the performance very much considering the standard deviation. It is also clearly visible that PDMS is regenerating to its original structure through time, just 15 minutes after the plasma process the water contact angle was back at 50% of its original angle, which leads to the conclusion that all further processes have to happen immediately after the plasma process to get the highest possible number of –OH groups on the surface.

The second plasma process was performed at **100% 20sccm of O$_2$ for 2 and 5 minutes** as shown in Table 29 and Figure 51.

Table 29: Water contact angles after plasma process with 100% and 20 sccm of O$_2$

| Time [min] | 0 | 15 | 30 |
|---|---|---|---|
| reference | 103.9° ± 5.3 | | |
| 2min exposed to plasma gas | 28.3° ± 3.6° | 51.8° ± 8.4° | 73.1° ± 9.4° |
| 5min exposed to plasma gas | 24.5° ± 7.6° | 38.1° ± 6.4° | 58.5° ± 8.2° |
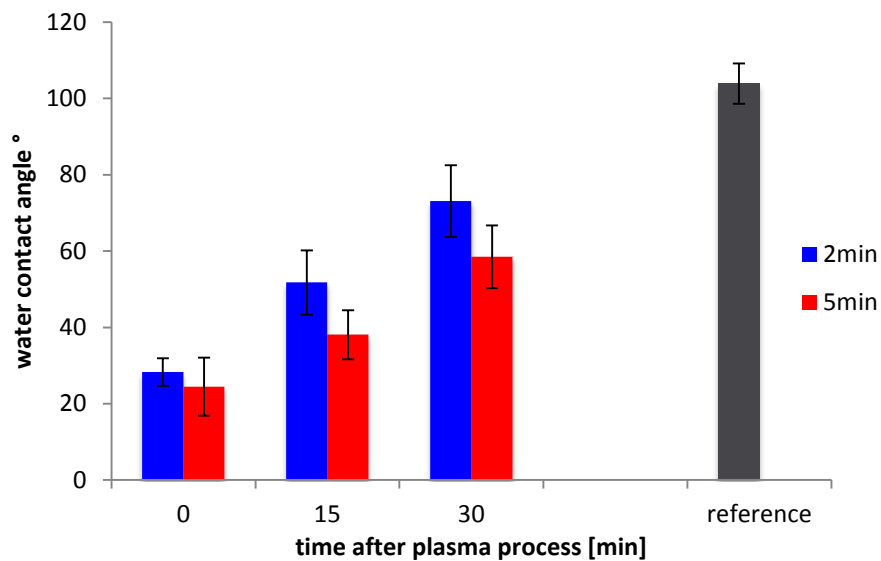


Figure 51: Water contact angles after plasma process with 100% and 20 sccm of O$_2$

With 20 sccm of O$_2$ the same results as mentioned above are achieved. There is a slight difference in the contact angles, and also in the regeneration time of PDMS. The smaller contact angle are probably due to more –OH groups on the surface resulting from a higher oxygen concentration in the plasma gas chamber.. This could also be the explanation for the longer regeneration time, if there are more –OH groups on the surface it takes longer that the –CH$_3$ groups of the inner layer of PDMS diffuse up to the surface.

The results show that the plasma process is a good way to activate a PDMS surface. The introduction of –OH groups onto the surface changes the properties from hydrophobic to hydrophilic, which is clearly indicated by the results of the water contact angle measurement. As you can see in Figure 52 the difference between the angles treated which different plasma gas settings is small, but there is a slight trend that the angle decreases with longer exposure time and increasing sccm of $O_2$. There is also a clear indication that PDMS regenerates fast after the treatment, so it is desirable that continuing reactions happen immediately after the plasma treatment. In Literature similar effects after the plasma treatment are reported [44].

For further experiments, following plasma gas settings were used: **100% 20sccm for 5 minutes** to make sure the highest number of active groups are available on the surface for further reactions.
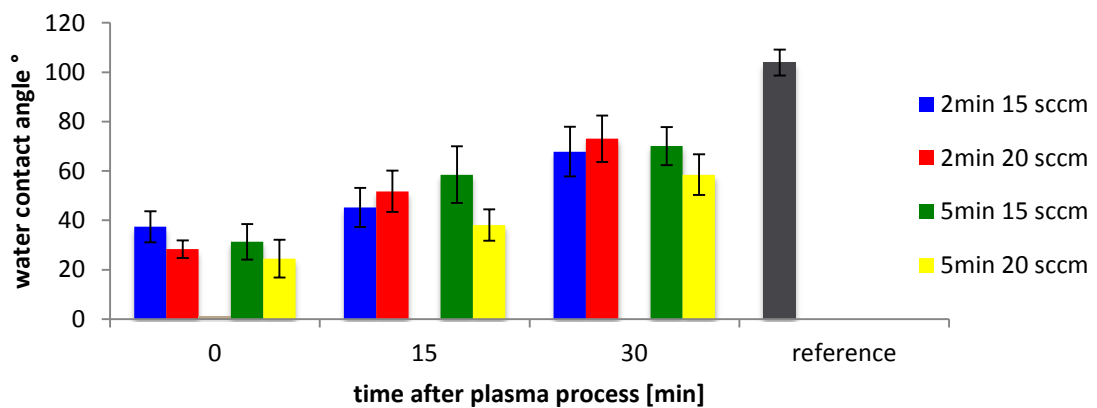


Figure 52: Comparison of water contact angles after two different plasma processes

In Figure 53 and Figure 54 photos made by the camera attached to the WCA machine are shown. Figure 53 shows the water drop on an untreated PDMS sample and Figure 54 shows the water drop on a PDMS sample after the plasma process.
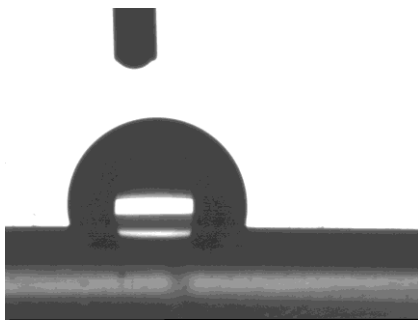


Figure 53: Water drop on untreated PDMS. Water contact angle approx. 103°
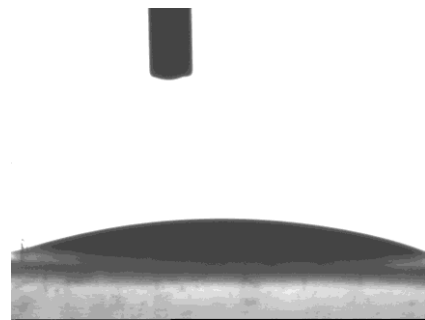
Figure 54: Water drop after plasma treatment on PDMS. Contact angle approx. 28°

### 3.2.3  APTES silanization of plasma treated PDMS

Immediately after PDMS samples were exposed to the plasma gas, they were given into APTES solutions describes in chapter 2.3.3. After incubation a ninhydrin test was performed to prove that there are $-NH_2$ groups on the PDMS surface. In Figure 55 a ninhydrin test is shown where the sample was inserted into an eppendorf tube and in Figure 56 the sample was sprayed on with the ninhydrin solution. As reference an untreated silicone plate was taken.



Figure 55: Ninhydrin test of APTES treated PDMS in an eppi
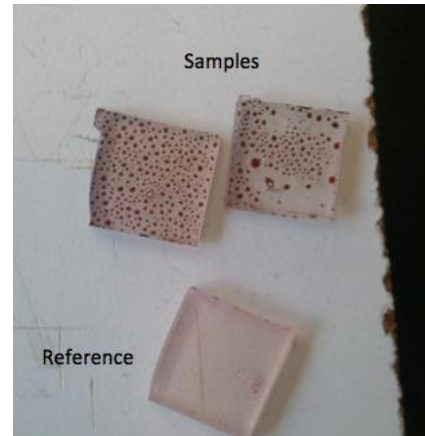


Figure 56: APTES treated PDMS sprayed on with ninhydrin solution

The color change from blue to red indicates that there are amine groups on the surface and the APTES silanization worked. Unfortunately it was not possible to quantify the results due to the fact that spectrophotometer is not capable of detecting color changes on solid samples. The different incubations times (10min and 24h) did not show a visible effect at this stage, but later on at the actual enzyme immobilization the samples with 10 min incubation times did not show any activity. All samples in following chapters had an APTES incubation time of 24h.

The next step was the attachment of glutaraldehyde onto the created amine groups, again the APTES treated samples were transferred immediately into the glutaraldehyde solution.

### 3.2.4 Use of glutaraldehyde as a crosslinker

Glutaraldehyde was used as a crosslinker between the APTES treated silicone plate and CDH. Different concentrations were used. There was no method known for analyzing aldehyde groups on a surface, but after approx. 10 minutes of incubation, it was clearly visible to the naked eye that glutaraldehyde was accumulating on the surface independent of the concentration. A red "film" was observed increasing in intensity with longer incubation time. Examples are shown in Figure 57.
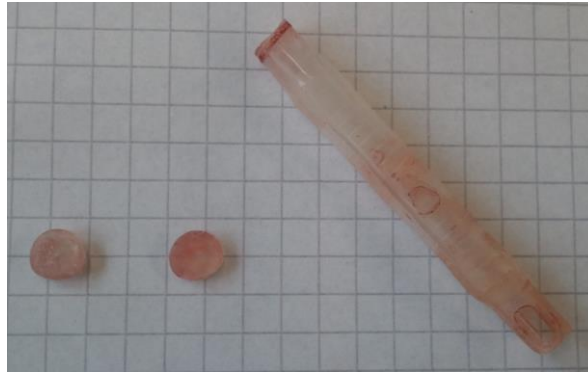


**Figure 57: Glutaraldehyde accumulated on silicone**

Not only the apparent evidence but also the successful enzyme immobilization described in the next chapter, are proof that the crosslinking with glutaraldehyde worked.

### 3.2.5 Cellobiose Dehydrogenase Immobilization

The final step of this immobilization process was the actual enzyme immobilization. Different immobilization conditions were tested and analyzed. The $H_2O_2$ production was the most valuable factor to compare results. The use of different glutaraldehyde concentrations as shown in table 30 and figure 59.

Table 30 and Figure 58 show the $H_2O_2$ production of CDH on PDMS crosslinked with different glutaraldehyde concentrations.

Table 30: $H_2O_2$ production of CDH on PDMS with different glutaraldehyde concentrations

| Glutaraldehyde concentration [w/v] | $H_2O_2$ [µM] |
|---|---|
| 0.5% | 1.3 ± 0.05 |
| 10% | 2.3 ± 0.8 |
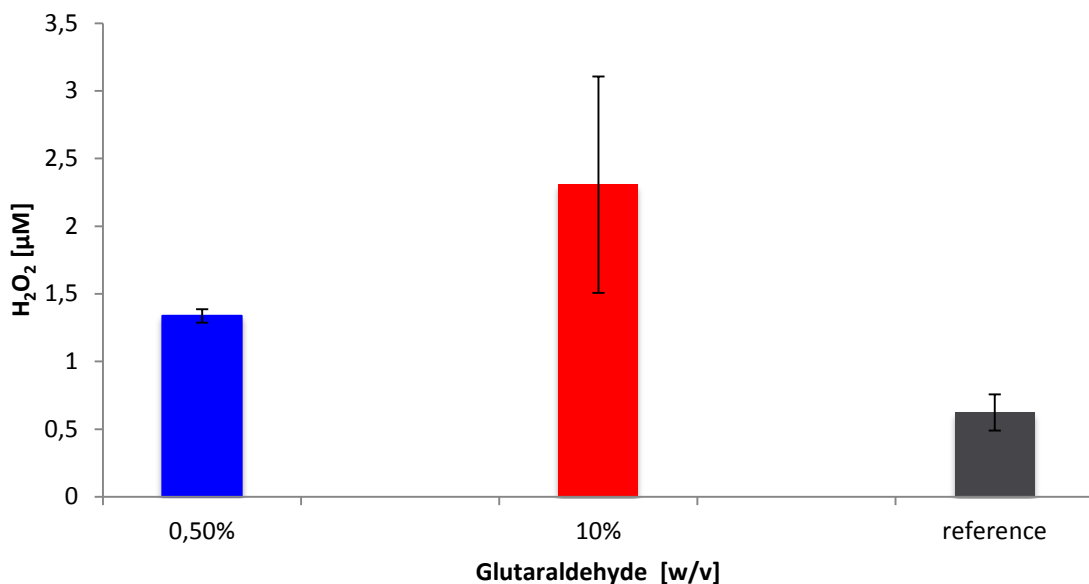


Figure 58: $H_2O_2$ production of CDH on PDMS with different glutaraldehyde concentrations

Crosslinking with a 10% [w/v] solution resulted in a higher production of $H_2O_2$ (**2.3 ± 0.8 [µM]**), which could be caused by a higher enzyme concentration linked to the surface. It seems that the saturation of glutaraldehyde on free amine groups from APTES is higher when more glutaraldehyde is available in the solution. With a 0,5% solution it seems that there are still free amine groups available. In the big picture this results in a higher CDH concentration because of more aldehyde groups to available for crosslinking. There was also a measurement with a 5% glutaraldehyde solution, but for reasons that are not reproducible the $H_2O_2$ concentration resulted in a negative value, and is not shown in the table or the graph. All further experiments were executed with a 10% glutaraldehyde solution.

The pH value plays an important role in enzyme immobilization. It distributes charges across the protein and changes its conformation.   To see which consequences the pH has on CDH, the immobilization process was executed at different pH values, illustrated in Table 31 and Figure 59.

Table 31: $H_2O_2$ production of CDH on PDMS at different pH values

| pH | $H_2O_2$ [µM] |
|---|---|
| 5.5 | 3.3 ± 2.3 |
| 6 | 2.3 ± 0.4 |
| 7.3 | 2.3 ± 1.1 |
| 8 | 5.9 ± 0.3 |
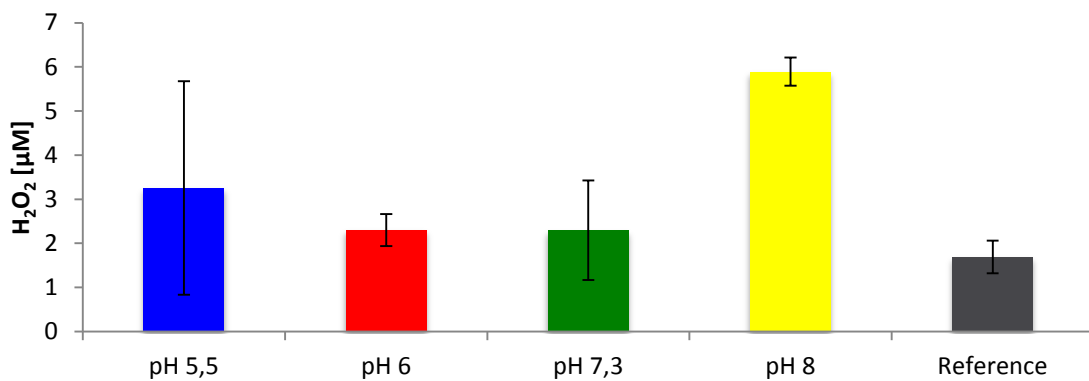


Figure 59: $H_2O_2$ production of CDH on PDMS at different pH values

CDH produced the highest amount of $H_2O_2$ at pH 8, which is also comparable to the optical oxygen meter measurement of the free enzyme in section 3.1.1. The slight alkaline environment is preferred by CDH and results, also in its immobilized state, in the highest activity. The measurement at pH 5.5 is a spike because of the high standard deviation. Due to the fact that this measurement was one of the last ones in this project the result was no used in further immobilizations. The immobilization in the next chapter was executed with pH 7.3.

Due to the fact that proteins are dynamic molecules and are able to change their properties, conformation or reaction rate with their surrounding environment, different immobilization conditions were tested. The temperature was set at 4°C to reduce the movement of the enzyme and also enhance its stability. The purpose was that if the enzyme moves less and does not change its inner structure. It is expected that the enzymes are immobilized the same way. Another approach was to immobilize CDH with its substrate cellobiose in the solution. The ambition was that with this method the active center is occupied by cellobiose, and reduces the possibility that CDH binds with its active center to the surface. A higher activity is expected. The enzyme concentration was also varied, to cover  a wide range 0.5 mg/ml and 7 mg/ml were used. This should conclude how many

active groups are on the surface and if there is a higher immobilization rate if more enzyme is available. The results are shown in Table 32 and Figure 60.

Table 32: $H_2O_2$ production with different immobilization conditions

| Conditions | $H_2O_2$ [µM] |
|---|---|
| 0.5 mg/ml CDH at 4° | 3.8 ± 0.3 |
| 0.5 mg/ml CDH at 4° + 10mM CB | 3.8 ± 0.8 |
| 7 mg/ml CDH at 4° | 3.8 ± 1.7 |
| 7 mg/ml CDH at 4° + 10mM CB | 4.4 ± 1.9 |
| Reference | 0.6 |
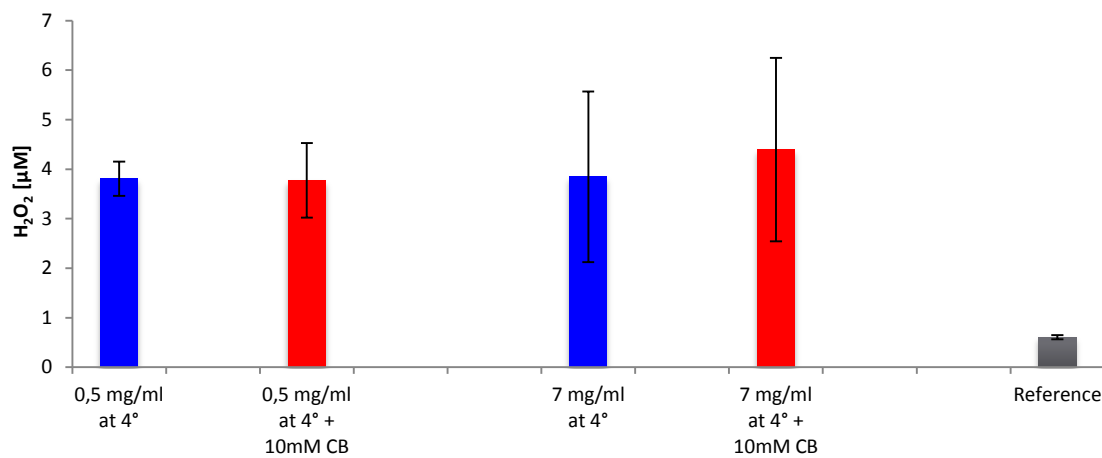


Figure 60: $H_2O_2$ production with different immobilization conditions

Unfortunately there was no significant effect on the $H_2O_2$ production of CDH after immobilization with different conditions. As there is no difference in the $H_2O_2$ production when different enzyme concentrations are used, it can be suggested that the number of active groups on the surface is limited to an amount that is already saturated with 0.5 mg/ml. Only the standard deviation increases with an enzyme concentration of 7 mg/ml, but there is no feasible explanation for that effect. The addition of cellobiose thus proved that groups of the enzyme which interact with the activated surface are not part of the active center. Otherwise there should be a difference in the activity between the samples with available cellobiose compared to the samples with none.

**FTIR surface analysis**

FTIR analysis, illustrated in in Figure 61, Figure 62 and Figure 63 clearly shows a modification of PDMS. Circles mark important sections in the spectrum. Descriptions of the names in the spectrum are illustrated in Table 33. The reference was an untreated PDMS plate.

Table 33: Description of names in the FTIR spectrum

| Name | Sample |
|---|---|
| 1 | 0.5 mg/ml CDH at 4° |
| 2 | 0.5 mg/ml CDH at 4° + 10 mM CB |
| 3 | 7 mg/ml CDH at 4° |
| 4 | 7 mg/ml CDH at 4° + 10 mM CB |
| Reference | Reference |
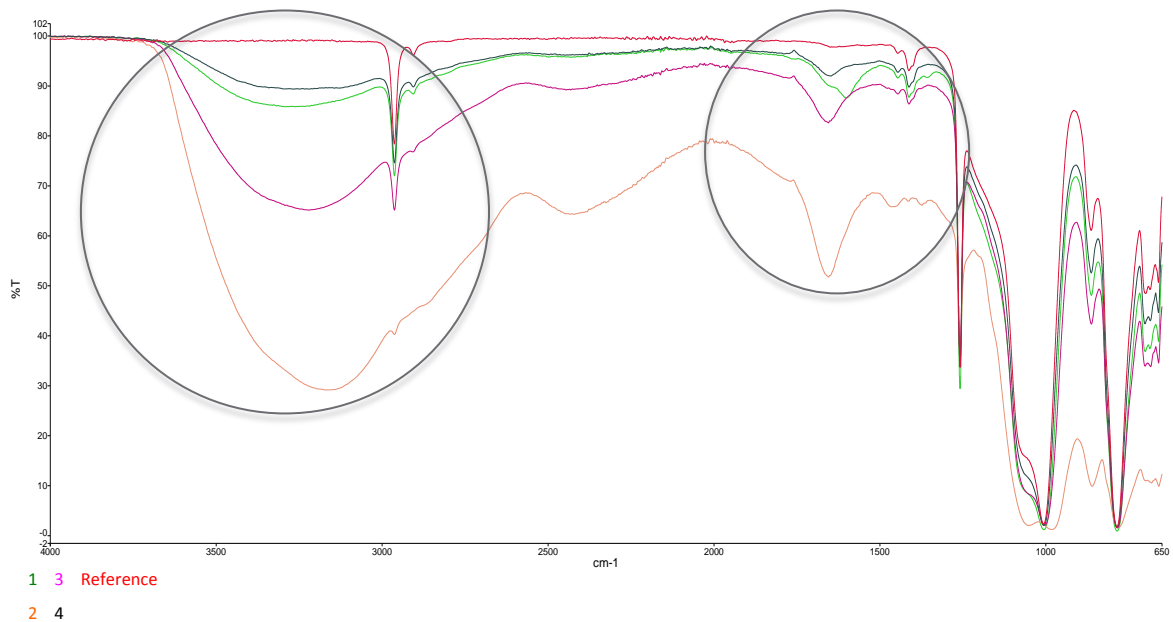


Figure 61: FTIR spectrum of CDH immobilized on PDMS with different conditions
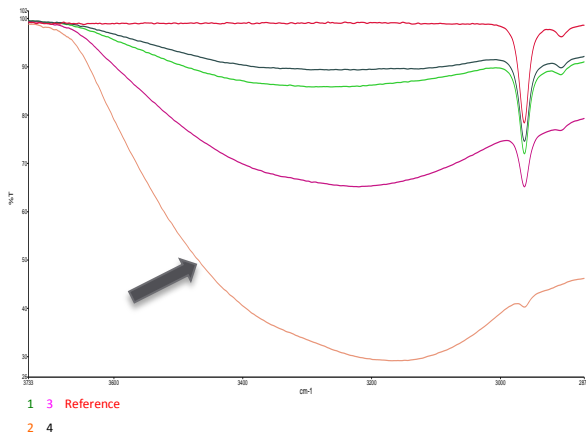
Figure 62: FTIR peaks of hydrogen bonds of CDH immobilized on PDMS with different conditions
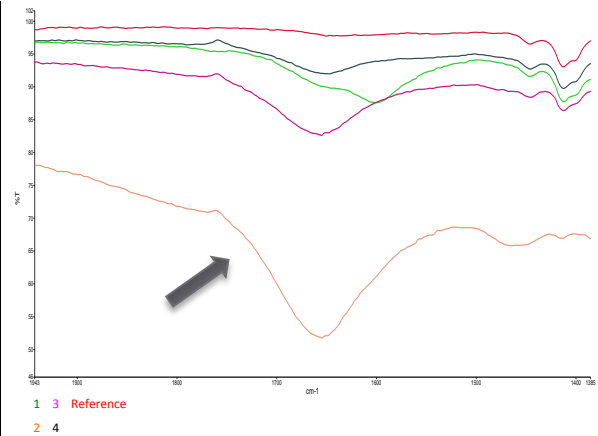


Figure 63: FTIR peaks of amide bonds of CDH immobilized on PDMS with different conditions

The spectrum shows that there is a significant difference between the samples and the reference. The -OH peak of 2 and 3 are big and kind of swallow the other peaks in the spectrum. One amide peak is also clearly visible, the second one is also kind of swallowed. As described in section 0 FTIR is a point measurement, and the distribution of immobilized CDH on the surface is diverse. Because of this, the peaks which differ in their plain size, do not correspond with the measured activities in the section above where all activities are almost the same. It is also not possible to define a system with this analysis. The main point of this FTIR measurement is the proof that there is CDH on the surface of PDMS and this is indicated very clearly.

The last step of this immobilization process was a success. All experiments worked and the conditions were optimized to get the best result. The $H_2O_2$ production after 5 minutes of CDH immobilized on silicone which was treated with a 10% [w/v] Glutaraldehyde solution at pH 7.3 and room temperature resulted in **2.3 ± 0.8 µM.** The same result was obtained in the next experiment with the same conditions, which resulted **2.3 ± 1.1 µM.** This result is also a proof of concept. With pH 8 the highest $H_2O_2$ production (**5.9 ± 0.3 µM)** was recorded. Unfortunately this result wasn't used for further experiments. The main difference in the immobilization process was the change of temperature. At 4°C CDH produced **3.8 ± 0.3 µM** of $H_2O_2$ compared to **2.3 ± 0.8 µM** with the same conditions at room temperature. Lastly the enzyme concentration was varied: **0.5, 1, 3 and 7 mg/ml** of CDH were used. There was no significant difference between 0.5 mg/ml and 7 mg/ml with the same conditions, and there was also no difference between **1 mg/ml and 3 mg/ml** with the same conditions. This concludes that there was an amount of active groups on the surface which where already saturated with **0.5 mg/ml.** With these results the optimal conditions for CDH immobilization are offered in Table 34.

**Table 34: Optimal CDH immobilization conditions**

|  | Value |
|---|---|
| Glutaraldehyde solution | 10% [w/v] |
| CDH concentration | 0.5 [mg/ml] |
| Temperature | 4 ° C |
| pH | 8 |

It is also reported that a similar protein of CDH, the glucose oxidase was immobilized with APTES onto different supports. Though the crosslinking process with glutaraldehyde was difficult to perform[45]. The addition of glucose to the immobilization to occupy the active center is also reported with positive results[46]. The optimal coupling conditions for glucose oxidase occur above pH 6[47].

### 3.2.6 Visualization of immobilized CDH

To further confirm our results FITC labeling was performed. To visualize that CDH is linked onto the surface of silicone, the enzyme was labeled with FITC and then immobilized. The immobilization conditions were the same as described oben Because FITC has the highest fluorescent emission in an alkaline environment one immobilization was carried out at pH 9. It was unclear if the enzyme binds the same way as described in the sections above. For security, the labeling was also carried out at pH 7.3 with a lower fluorescent signal expected. The fluorescent images shown in Figure 64 and Figure 65 were taken on a BIO RAD Chemidoc with an exposure time of 0.182 seconds.
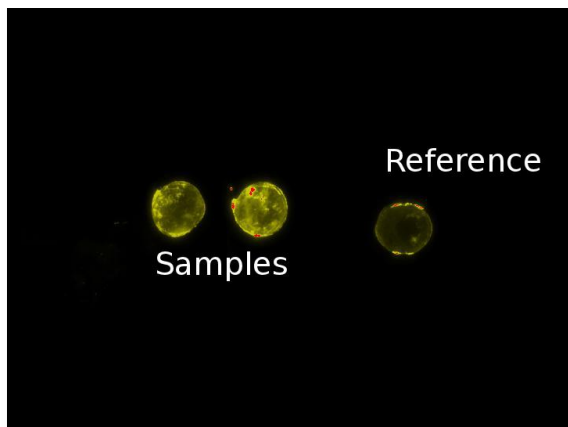


**Figure 64: Image of FITC labeled CDH immobilized at pH 9**
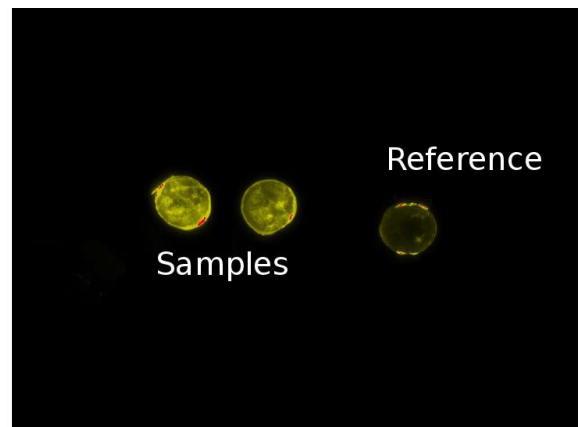


**Figure 65: Image of FITC labeled CDH immobilized at pH 7.3**

The images in Figure 64 and Figure 65 illustrate an expected outcome: It is a clear proof that CDH is linked to the surface of PDMS. The intensity of fluorescent signal is higher in Figure 64 at pH 9, which results out of the higher emission of FITC at pH 9. CDH immobilized at pH 7.3 shows a wider distribution on the surface and concludes a higher enzyme concentration (Figure 65).

# 4   Conclusion and Outlook

The aim of this work was to investigate the possibility of immobilizing *cellobiose dehydrogenase* on silicone (PDMS). Silicone is the most widely used material for urinary catheters but also a favored material by bacteria to form biofilms on it causing infections. To prevent these infections CDH was immobilized onto the surface of PDMS to produce an antibacterial catheter based on formation of hydrogen peroxide.

In this thesis different immobilization techniques were employed, analyzed and compared.

The first method to bind CDH to the surface of PDMS was the layer by layer approach. FTIR results indicate with two significant peak changes, that there is an interaction of CDH with the surface. CDH clearly binds to the PDMS surface, nevertheless an expected bilayer built up with chitosan was not achieved, revealed by FTIR spectra with chitosan as the first layer and the Surpass measurement also confirmed this conclusion. The expectation that chitosan acts as a polycation was wrong. Activity assay of the treated silicone plates also showed positive results. The $H_2O_2$ production was moderately after 3 hours of incubation and resulted in values from **3.8 to 14.4 µM** dependent on the time the PDMS plates were exposed to the CDH solution**.** The outcome of the layer by layer technique is promising, but optimization is needed, for example another polycation has to be tried, to really built up bilayers. This would increase the stability of layers and also would result in a higher enzyme concentration on the surface.

The introduction of hydroxyl groups on to the silicone surface with piranha solution did not work. After incubation of the samples in the solution, there was just a visible effect on the surface of PDMS but all measurements for activation showed no difference compared to references. The structure of finished polymerized  silicone is very difficult to attack, also by the highly oxidative piranha solution.

Activation the surface of PDMS with plasma gas was successful. The water contact angle after the plasma treatment changed from approx. **103°** to approx. **25°**, therefore the surface changed its properties from hydrophobic to hydrophilic. The oxygen gas introduced –OH groups to the surface. The fast regeneration of PDMS was another observed effect after the plasma treatment.  After 30 minutes the contact angle was back at about 50% of its original angle.

The amine group content determination via a ninhydrin test was successful and proved that APTES was linked to the activated surface. The visible change of the surface after the glutaraldehyde solution also indicates that the APTES treatment worked and that glutaraldehyde accumulated onto the surface. The successful immobilization of CDH also indicates that those two steps worked.

The final immobilization of CDH onto the activated surface also showed positive results. Not only was proved that the enzyme is still active on the surface by an $H_2O_2$ assay, but also a FTIR measurement on the surface of treated PDMS plates showed clear visible peaks which indicate an successful immobilization. The covalent bonding of the enzyme resulted in a higher activity than the interaction with layer by layer technique. After just **5 minutes** of incubation with its substrate,CDH produced **3.8 ± 0.3 µM** $H_2O_2$ when covalent bound to the surface, compared to the **14.4 µM** $H_2O_2$ produced by CDH interacting with the surface, after **3 hours** of incubation.

The successful immobilization with FITC labeled CDH was the last experiment in this thesis. The samples showed a clear fluorescent signal and indicate that the immobilization of CDH onto the surface of PDMS was successful through all stages.

This thesis is a proof of concept that it is possible to bind CDH onto the surface of silicone. The successful immobilization is the first step in creating an antibacterial catheter. But there is still a lot of work to do until the first antibacterial catheter will be inserted into a patient. The next steps will have to tackle the optimization of this whole process. It will be necessary to be able to introduce more active groups to the surface of PDMS, then it will be able to immobilize more enzyme, which will increase the $H_2O_2$ production and the ability to prevent biofilm formation. Another approach would be to activate PDMS at the stage of polymerization. Due to the fact that the body depletes foreign proteins, there is also a protection layer needed, before insertion. An option could be a membrane like layer, where only cellobiose is able to diffuse in, and only small molecules like $H_2O_2$ are able to diffuse out. Finally, compatibility of immobilized enzymes with medical devices regarding registration has to be considered.

A lot of research, studies and experiments have to be made but the future for implementation of an antibacterial catheter looks promising.

# 5   Declaration

## EIDESSTATTLICHE ERKLÄRUNG

Ich erkläre an Eides statt, dass ich die vorliegende Arbeit selbstständig verfasst, andere als die angegebenen Quellen/Hilfsmittel nicht benutzt, und die den benutzten Quellen wörtlich und inhaltlich entnommene Stellen als solche kenntlich gemacht habe.

Graz, am …………………………                    …………………………………………….

                                                     (Unterschrift)

## STATUTORY DECLARATION

I declare that I have authored this thesis independently, that I have not used other than the declared sources / resources, and that I have explicitly marked all material which has been quoted either literally or by content from the used sources.

…………………………                       …………………………………………….

         date                                          (signature)

# 6   References

1. NOVO Project: Development of tools to control microbial biofilms with relevance to clinical drug resistance Grant agreement for : Collaborative project Annex I. 2011.

2. Hall-Stoodley, L., Costerton, J., W. & Stoodley P. Bacterial biofilms: from the natural environment to infectious diseases. *Nat. Rev. Microbiol*. 2004;2:95–108.

3. Costerton, J., W., Stewart, P.S. & Greenberg E. Bacterial biofilms: a common cause of persistent infections. *Science (80-. ).* 1999;284:1318–1322.

4. Fux, C., A., Stoodley, P., Hall-Stoodley, L. & Costerton JW. Bacterial biofilms: a diagnostic and therapeutic challenge. *Expert Rev. Anti. Infect. Ther*. 2003;1:667–683.

5. Stamm, W. E. Catheter-associated urinary tract infections: epidemiology, pathogenesis, and prevention. *AM. J. Med.* 1991;91:65S–71S.

6. Morris, N., S., Stickler, D., J., & McLean, R. J. The development of bacterial biofilms on indwelling urethral catheters. *World J. Urol*. 1999;17:345–350.

7. Pricelius S, Ludwig R, Lant N, Haltrich D. Substrate specificity of Myriococcum thermophilum cellobiose dehydrogenase on mono- , oligo- , and polysaccharides related to in situ production of H 2 O 2. 2009:75–83.

8. Henriksson G, Pettersson G, Johansson G, Ruiz A UE. Cellobiose oxidase from Phanerochaete chrysosporium can be cleaved by papain into 2 domains. *Eur J Biochem*. 1991;196:101–106.

9. Henriksson G, Johansson G, Pettersson G. A critical review of cellobiose dehydrogenases. *J. Biotechnol.* 2000;78(2):93–113. Available at: http://www.ncbi.nlm.nih.gov/pubmed/10725534.

10. Eriksson, K.E., Blanchettete, R.A. AP. Microbial and Enzymatic Degradation of Wood and Wood Components. *Springer Verlag*. 1990.

11. Hall-Stoodley L, Costerton JW, Stoodley P. Bacterial biofilms: from the natural environment to infectious diseases. *Nat. Rev. Microbiol.* 2004;2(2):95–108. Available at: http://www.ncbi.nlm.nih.gov/pubmed/15040259. Accessed August 7, 2013.

12. Monroe D. Biofilms, Looking for Chinks in the Armor of Bacterial. *PLoS Biol.* 2007;5(11):2458–2461.

13. Parsek MR, Singh PK. Bacterial biofilms: an emerging link to disease pathogenesis. *Annu. Rev. Microbiol.* 2003;57:677–701. Available at: http://www.ncbi.nlm.nih.gov/pubmed/14527295. Accessed August 8, 2013.

14. Bryers JD. Medical biofilms. *Biotechnol. Bioeng.* 2008;100(1):1–18. Available at: http://www.pubmedcentral.nih.gov/articlerender.fcgi?artid=2706312&tool=pmcentrez&rendertype=abstract. Accessed August 10, 2013.

15. Hoffman AS, Hubbell JA. *Chapter I.2.17 – Surface-Immobilized Biomolecules*. Third Edit. Elsevier; 2009:339–349. Available at: http://dx.doi.org/10.1016/B978-0-08-087780-8.00032-2.

16. Tischer W, Wedekind F. Immobilized Enzymes : Methods and Applications. 1999;200.

17. Jastrz M. Immobilization techniques and biopolymer carriers. 2011;75(1):65–85.

18. A.S. H. Modification of material surfaces to affect how they interact with blood. *Ann. NY Acad Sci.* 1987;516:96–101.

19. A.S H. Applications of plasma gas discharge treatments for modification of biomaterial surfaces. *J. Appl. Polym. Sci. Symp*. 1988;42:251.

20. Hoffman A.S., Gombotz, W.R., Uenoyama, S., Dong, L.C., & Schmer G. Immobilization of enzymes and antibodies to radiation grafted polymers for therapeutic and diagnistic applications. *Radiat. Phys. Chem.* 1986;27:256–273.

21. Catheters J, Ages M. History of catheters. 2011:475–477.

22. Lawrence EL, Turner IG. Materials for urinary catheters : a review of their history and development in the UK. 2005;27:443–453.

23. Linear Polydimethylsiloxanes. *Jt. Assess. Commod. Chem.* 1994;26(0773-6339-26).

24. Biomaterials P. Historical Milestones in Silicone Chemistry. 1978:82–91.

25. Owen MJ. Why silicones behave funny. *Chemtech*. 1981;11:288.

26. Al S et. Silicones. *Compr. Organomet. Chem.* 2:288–297.

27. Curtis J. A Comparative Assessment of Three Common Catheter Materials.

28. Tang, Z. et al. Biomedical Applications of Layer-by-Layer Assembly: From Biomimetics to Tissue Engineering. *Adv. Mater.* 2006;18:3203–3224.

29. Ariga, K., Hill, J.P. and Ji Q. Layer-by-layer assembly as a versatile bottom-up nanofabrication technique for exploratory research and realistic application. *Phys. Chem. Chem. Phys.* 2007;9:2319–2340.

30. A G. Thin polymer films based on multilayer assemblies. *Nanoindustrija*. 2007;4:34–36.

31. Ratner BD, Hoffman AS. *SURFACE MODIFICATION OF Thin Surface Modifications Surface Rearrangement Surface Analysis Delamination Resistance Commercializability The end products of biomaterials research are devices*. Third Edit. Elsevier; :259–276. Available at: http://dx.doi.org/10.1016/B978-0-08-087780-8.00027-9.

32. Siow KS, Britcher L, Kumar S, Griesser HJ. Plasma Methods for the Generation of Chemically Reactive Surfaces for Biomolecule Immobilization and Cell Colonization - A Review. 2006:392–418.

33. Coupling S, Guide A. UCT Silane coupling agent guide. Available at: http://www.amchro.de/PDFs/Silane/Neu-SilaneCouplingAgents08.pdf. Accessed September 2, 2013.

34. Migneault I, Dartiguenave C, Bertrand MJ, Waldron KC. Glutaraldehyde : behavior in aqueous solution , reaction with proteins , and application to enzyme crosslinking. 2004;37(5).

35. Griffiths, Peter R. de HJA. *Fourier Transform Infrared Spectrometry 2nd ed*. Wiley-Blackwell; 2007.

36. FT-IR Spectroscopy Attenuated Total Reflectance (ATR). *Perkin Elmer Life Anal. Sci.* 2005. Available at: http://shop.perkinelmer.com/content/TechnicalInfo/TCH_FTIRATR.pdf. Accessed September 2, 2013.

37. F. M. Mirabella J. *Practical Spectroscopy Series; Internal reflection spectroscopy: Theory and applications*. marcel dekker inc; 1993:17–52.

38. Yuan Y, Lee TR. Surface Science Techniques. Bracco G, Holst B, eds. 2013;51. Available at: http://www.springerlink.com/index/10.1007/978-3-642-34243-1. Accessed August 7, 2013.

39. Sygmund et al. Semi-rational engineering of cellobiose dehydrogenase for improved hydrogen peroxide production. *Microb. Cell Fact.* 2013;12:38. Available at: http://www.microbialcellfactories.com/content/12/1/38.

40. Baminger U, Nidetzky B, Kulbe KD, Haltrich D. Short communication A simple assay for measuring cellobiose dehydrogenase activity in the presence of laccase. 1999;35:253–259.

41. Roti ® -Nanoquant - Instruction for use. Available at: http://www.carlroth.com/media/_nl-nl/usage/K880.pdf. Accessed September 5, 2013.

42. Constantine CA, Gatta KM, Mello S V, et al. Layer-by-Layer Films of Chitosan , Organophosphorus Hydrolase and Thioglycolic Acid-Capped CdSe Quantum Dots for the Detection of Paraoxon. 2003:13762–13764.

43. Maji D, Lahiri SK, Das S. Study of hydrophilicity and stability of chemically modified PDMS surface using piranha and KOH solution. *Surf. Interface Anal.* 2012;44(1):62–69. Available at: http://doi.wiley.com/10.1002/sia.3770. Accessed March 4, 2013.

44. Hong SM, Kim SH, Kim JH, Hwang HI. Hydrophilic Surface Modification of PDMS Using Atmospheric RF Plasma. 2006;656.

45. Bankar SB, Bule M V, Singhal RS, Ananthanarayan L. Glucose oxidase — An overview. *Biotechnol. Adv.* 2009;27(4):489–501. Available at: http://dx.doi.org/10.1016/j.biotechadv.2009.04.003.

46. Ozyilmaz G TS. Simultaneous co-immobilization of glucose oxidase and catalase in their substrates. *Appl Biochem Microbiol*. 2007;43(1):29–35.

47. Bouin J, Atallah M HH. Parameters in the construction of an immobilized dual enzyme catalyst. *Biotechnol Bioeng*. 1976;18:179–87.

# 7 Abbreviations

| | |
|---|---|
| CDH | cellobiose dehydrogenase |
| PDMS | polydimethylsiloxane |
| APTES | (3-Aminopropyl)triethoxysilane |
| GOPTMS | (3-Glycidyloxypropyl)trimethoxysilane |
| MPTMS | (3-Mercaptopropyl)trimethoxysilane |
| $dH_2O$ | destilled water |
| mQ- | milli Q |
| $H_2O_2$ | hydrogen peroxide |
| FAD | flavin adenine dincleotide |
| EtOH | ethanol |
| Fe | iron |
| Cu | copper |
| EPS | Extracellular polymeric substances |
| FITC | fluoresceinisothiocyanate |
| DNA | deoxyribonucleic acid |
| -OH | hydroxyl group |
| -COOH | carboxyl group |
| $H_2O$ | water |
| HCl | hydrochloric acid |
| $-NH_2$ | amino group |
| $-CH_3$ | methyl group |
| $SiO_2$ | silica |
| $O_2$ | oxygen |
| PDDA | poly(diallyldimethylammonium chloride) |
| PAH | poly(allylaminehydrochloride) |
| PEI | polyethyleneimine |
| CS | chitosan |
| $H_2SO_4$ | sulfuric acid |
| $H_2SO_5$ | caros's Acid |
| $H_3O^+$ | hydronium ion |
| $HSO_4^-$ | Bisulfate ion |
| Na | sodium |
| $NaPO_4$ | sodium phophate |
| UV | ultraviolet |
| RFGD | radio frequency glow discharge |
| FTIR | fourier transform infrared spectroscopy |
| WCA | water contact angle |
| ATR | attenuated total reflectance |
| Mt | myriococcum thermophilium |
| DCIP | 2,6 dichlorophenolindophenol |
| BCA | bicinchoninic acid |
| $Na_2CO_3$ | sodium carbonate |
| $NaHCO_3$ | sodium bicarbonate |
| KOH | potassium hydroxide |

| | |
|---|---|
| $KPO_4$ | potassium phosphate |
| Mhz | megahertz |
| IEP | isoelectric point |
| mbar | millibar |
| rpm | Revoluzions per minute |
| °C | degree celsius |
| % | percent |
| (w/v) | weight per volume |
| °C | degree Celcius |
| cm | centimeter |
| mm | millimeter |
| µm | micrometer |
| nm | nanometer |
| c | concentration |
| M | mole per liter |
| mg | milligram |
| min | minute |
| ml | milliliter |
| mM | millimole per liter |
| µM | micromole per liter |
| t | time |
| U | unit |
| U/mL | units per milliliter |
| ε | molar extinction coefficient |
| λ | wavelength |
| µL | microliter |
| µmol | micromol |

# 8  Equipment
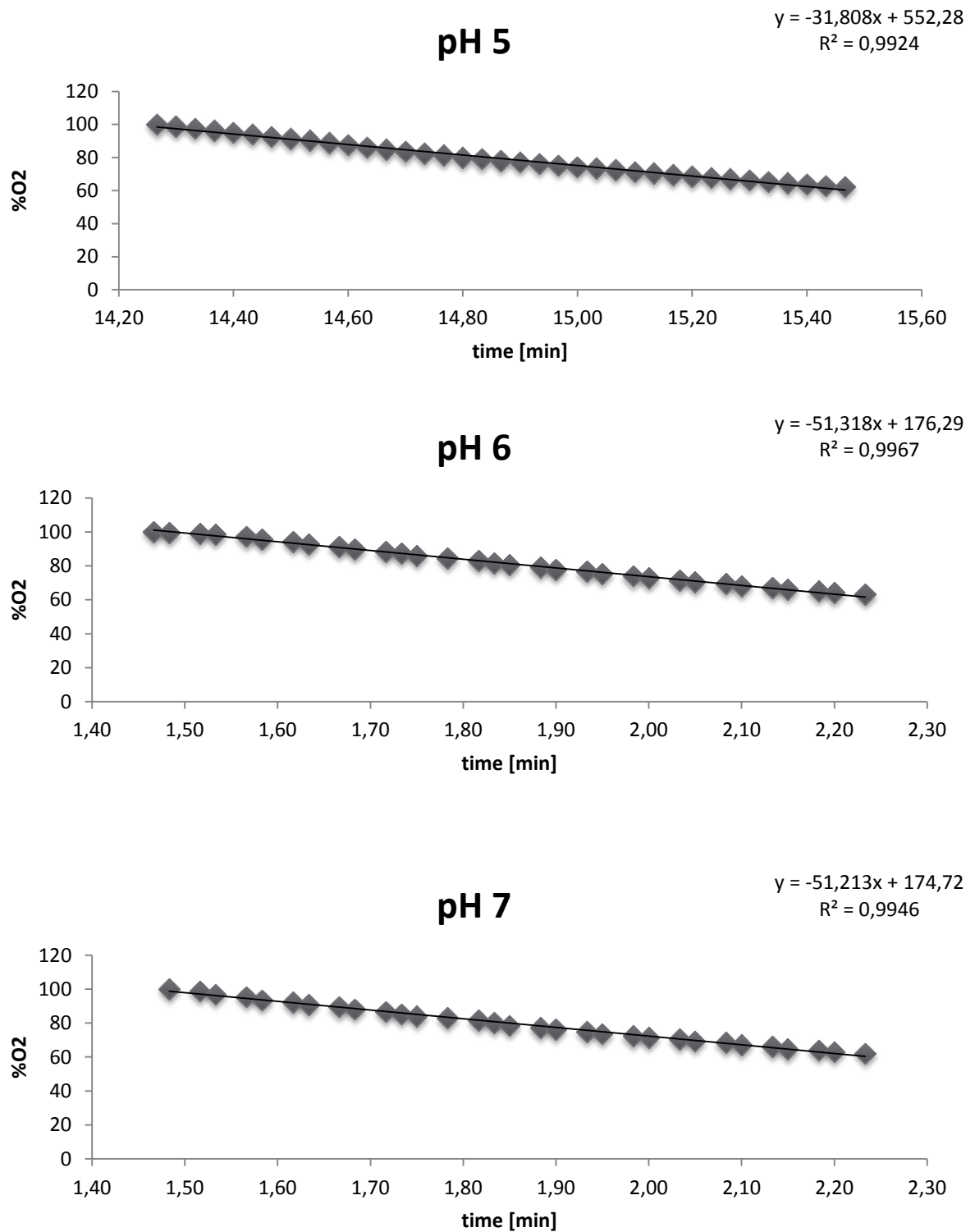
| | |
|---|---|
| AEKTA purifier | Amersham Pharmacia Biotech, Model |
| PLASMA equibment | Diener electronics  Femto (version 4) |
| Optical Oxygen meter | FireSting O2 Fiber-Optic Oxygen Meter |
| Imaging system | Bio RAD ChemiDoc Universal Hood III |
| FTIR Spectrometer | Perkin Elmer, Spectrum 100 |
| Water contact angle | Krüss DSA 100 |
| analytic balance | Sartorius 2004 MP |
| analytic balance | KERN PB |
| analytic balance | DENVER instrument, S-4002 |
| centrifuge | Eppendorf mini spin (F-45-12-11) |
| centrifuge | Hettich EB 3S |
| centrifuge | Heraeus, Biofuge primo |
| magnetic stirrer | IKA RCT basic |
| pH-meter | METTLER TOLEDO, Seven Easy |
| Photometer | HITACHI, Spectrophotometer U2001 |
| pipette | Carl Roth GmbH |
| pipette | Soccorex, ACURA 825 |
| plate reader | TECAN infinite M200 |
| thermomixer | Eppendorf Thermomixer comfort |
| vortex | JANKE & KUNKEL, IKA, VF2 |

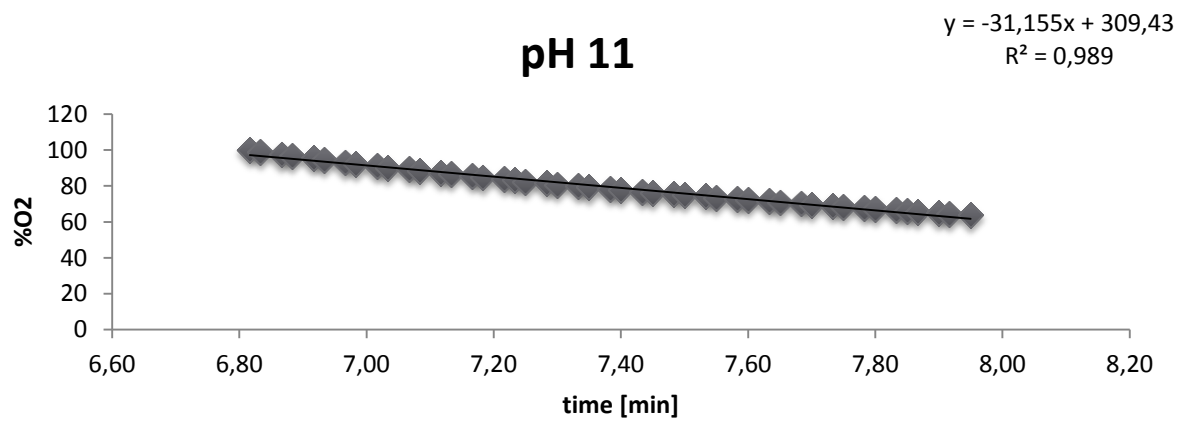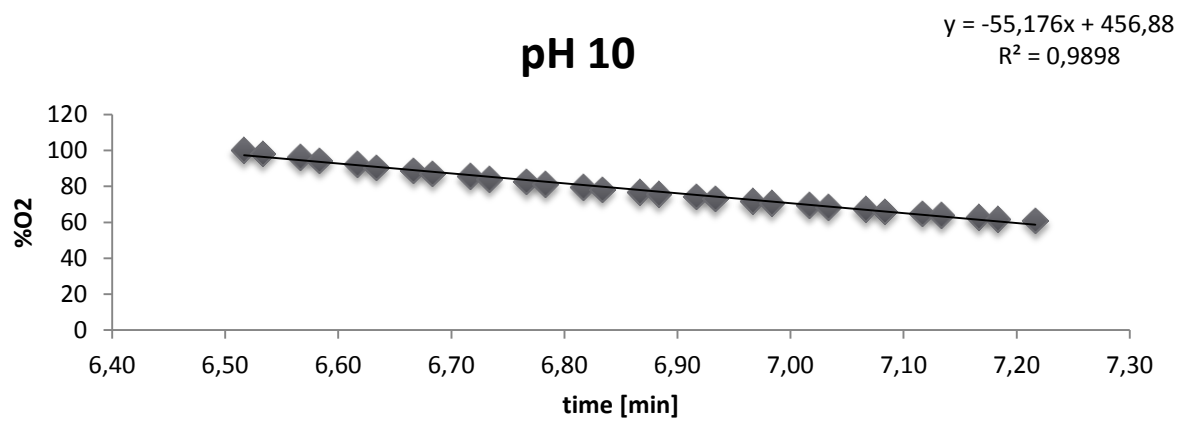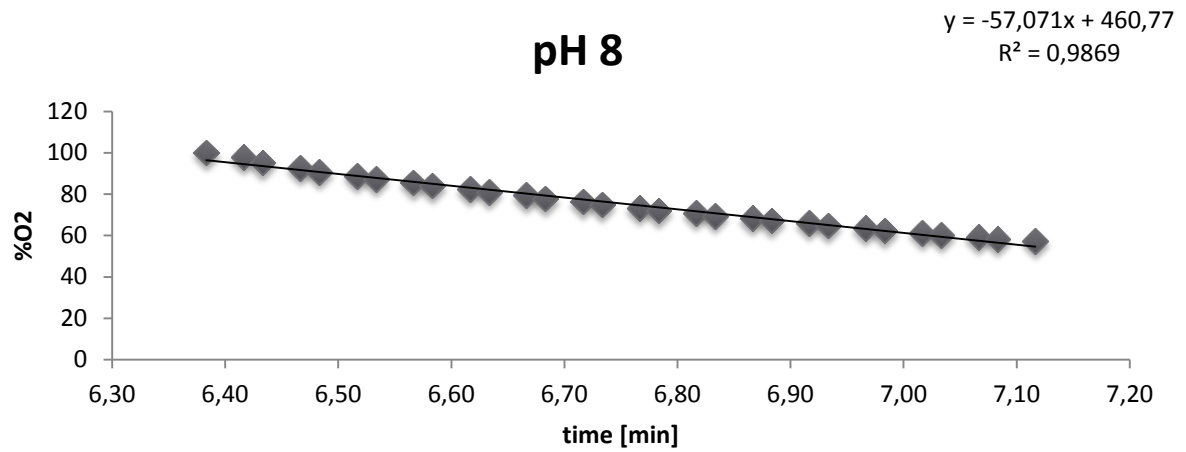# 9 Chemicals

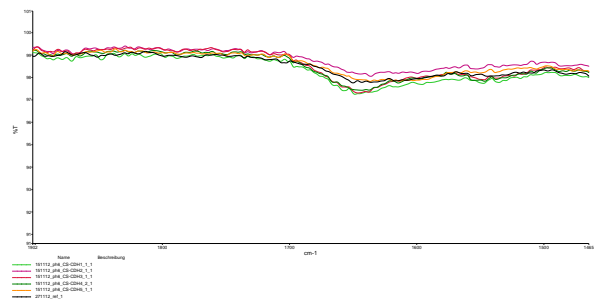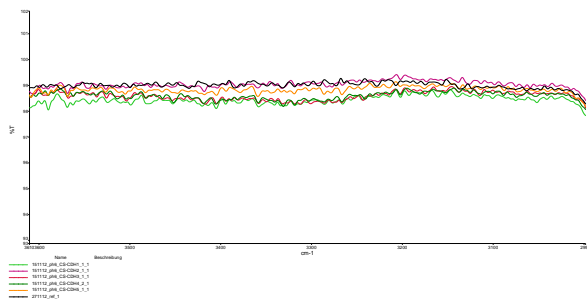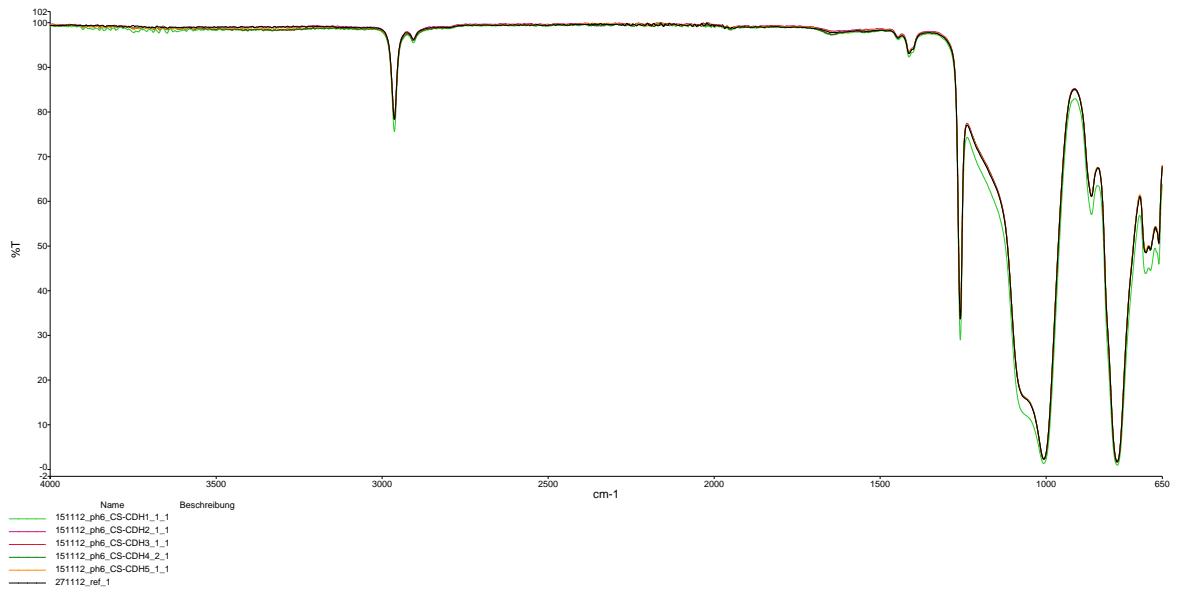| | |
|---|---|
| (3-Aminopropyl)triethoxysilane | Sigma Aldrich |
| Acetic acid | Carl Roth GmbH |
| Acetone | Carl Roth GmbH |
| Di-sodiumhydrogenphosphate dehydrate | Carl Roth GmbH |
| Ethanol | Carl Roth GmbH |
| Fluoresceinisothiocyanate | Sigma Aldrich |
| Hydrochloric acid | Carl Roth GmbH |
| Sodium citrate | Sigma Aldrich |
| Sodium carbonate anhydrate | Carl Roth GmbH |
| Sodium di-hydrogen phosphate 2-hydrate | Carl Roth GmbH |
| Cellobiose | Carl Roth GmbH |
| Lactose monohydrate | Carl Roth GmbH |
| 2,6-Dichlorophenolindophenol | Hoffman La Roce |
| Sodium chloride | Carl Roth GmbH |
| Hydrogen peroxide | Sigma Aldrich |
| Glutaraldehyde | Sigma Aldrich |
| 2-Propanol | Carl Roth GmbH |
| Bicinchoninic acid | EMD Millipore chemicals |
| Sulfuric acid | Merck |
| Human Serum Albumin | Sigma-Aldrich |
| Sodium hydroxide | Carl Roth GmbH |
| Potassium hydroxide | Carl Roth GmbH |
| Sodium cyanoborohydride | Sigma Aldrich |
| Dipotassium phosphate | Carl Roth GmbH |
| Monopotassium phosphate | Carl Roth GmbH |

# 10  Appendix

Optical oxygen meter Results for different pH values

$y = -31,808x + 552,28$
$R^2 = 0,9924$



$y = -51,318x + 176,29$
$R^2 = 0,9967$



$y = -51,213x + 174,72$
$R^2 = 0,9946$

pH 8

$y = -57,071x + 460,77$
$R^2 = 0,9869$

pH 10

$y = -55,176x + 456,88$
$R^2 = 0,9898$

pH 11

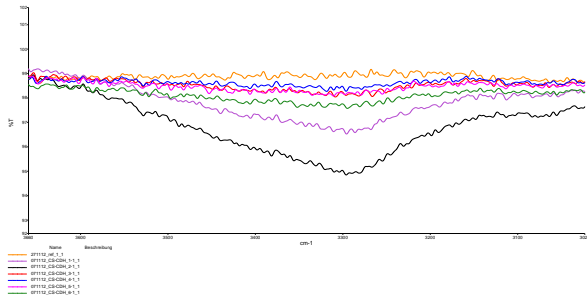$y = -31,155x + 309,43$
$R^2 = 0,989$

## Layer by layer spectra CS as first layer at pH 6



## pH 4 with Chitosan as first layer
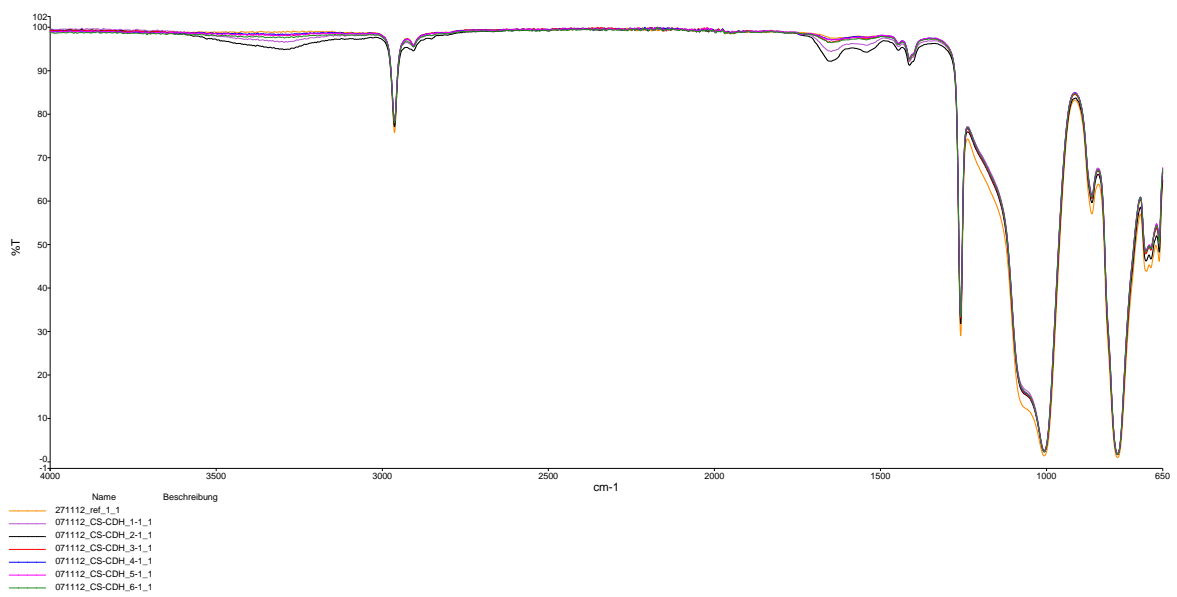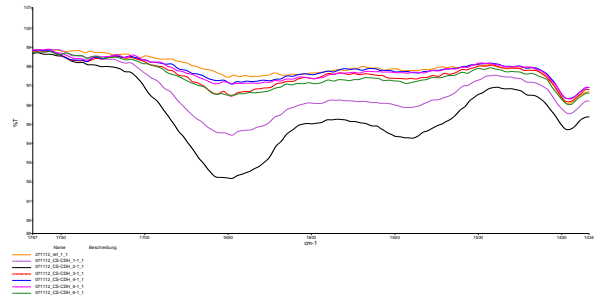
# 11 Acknowledgments

This thesis is dedicated to my Grandma **Trude Brandauer.**

I want to thank my professor **Georg Gübitz** for giving me the opportunity to complete this thesis, despite the times of change. Especially I want to thank **Barbara Thallinger** for her above ordinary supervision, but also for her motivating words and all the paroxysm of laughter every day which made it special. I also want to thank **Gibson Nyanhongo** for all his scientific knowledge, his tips, and his ideas throughout this thesis. Furthermore I want to thank **Klaus, Veronika, Doris, Tamara, Anne, Claudio, Stefan, Angi, Vanessa, Endry, Gamsi, Karolina, Armin** and the whole environmental biotechnology Institute for making this time memorable.

I want to thank my parents **Helga and Thomas** for being the best parents in the world, for all their assistance in every situation in life and making me the human I am today. I also want to thank my sister **Lena** for being there for me. Moreover I want to thank **Helmut, Hanni, Gudrun, Ulfrid, Hanno** and all the rest of **my family** for their support.

I want to thank **Kristof Grabmayer** for this continuous walk trough life, for all the conversations, and all the laughs since 1988. I also want to thank **Andi, Bernti, Sevi, Daniel, Grade, Lucas, Q, Angi, Marlene, Berni, Sabi, Hansi, Max, Börns, Markus, Armando** for all the good times we had together.

Thank you **Kati** for all your love and reminding me.

(I hope I did not forget anybody, but if so please feel as if you are on this list).

THANK YOU